ANKARA YILDIRIM BEYAZIT UNIVERSITY GRADUATE SCHOOL OF NATURAL AND APPLIED SCIENCE

REMOVING METAL IONS FROM THE SOLUTION OF ELECTROPOLISHED KOVAR ALLOY

M.Sc. Thesis by

SİDAL YAĞMUR

Department of Materials Engineering

November, 2024

ANKARA

REMOVING METAL IONS FROM THE SOLUTION OF ELECTROPOLISHED KOVAR ALLOY

A Thesis Submitted to

The Graduate School of Natural and Applied Sciences of

Ankara Yıldırım Beyazıt University

In Partial Fulfillment of the Requirements for the Degree of Master of Science in Materials Engineering, Department of Materials Engineering

by

Sidal YAĞMUR

November, 2024

ANKARA

M. Sc. THESIS EXAMINATION RESULT FORM

We have read the thesis entitled **"REMOVING METAL IONS FROM THE SOLUTION OF ELECTROPOLISHED KOVAR ALLOY"** completed by **Sidal YAĞMUR** under supervision of **Assoc. Prof. Dr. Metehan ERDOĞAN** and we certify that in our opinion it is fully adequate, in scope and in quality, as a thesis for the degree of Master of Science.

Assoc. Prof. Dr. Metehan ERDOĞAN

Supervisor

Asst. Prof. Dr. Begüm ÜNVEROĞLU

Jury Member

Assoc. Prof. Dr. Fuat ERDEN

Jury Member

Prof. Dr. Sadettin ORHAN

Director

Graduate School of Natural and Applied Sciences

ETHICAL DECLARATION

I hereby declare that all information in this document has been obtained presented in accordance with academic rules and ethical conduct. I have fully cited and referenced all material and results that are not original to this work.

I hereby declare that, in this thesis which has been prepared in accordance with the Thesis Writing Manual of Institute of Science and Technology,

- All data, information and documents are obtained in the framework of academic and ethical rules,
- All information, documents and assessments are presented in accordance with scientific ethics and morals,
- All the materials that have been utilized are fully cited and referenced,
- No change has been made on the utilized materials,
- All the works presented are original,

and in any contrary case of above statements, I accept to renounce all my legal rights.

Date: 25.11.2024 **Signature:**

Name & Surname: Sidal YAĞMUR

ACKNOWLEDGEMENTS

I would like to express my deepest gratitude to my thesis supervisor Assoc. Prof. Dr. Metehan ERDOĞAN, for his expertise, professionalism, helpful guidance, motivation and contributions in the process of the realization of this study, patience and support throughout my studies.

Besides the supervisor who is Assoc. Prof. Dr. Metehan ERDOĞAN, I would like to thank Esra KARAKAYA and Prof. Dr. İshak KARAKAYA, who opened his laboratory to me and allowed to use all his opportunities.

Moreover, special thanks should be given to Büşra Kozan for her motivation.

I would like to express my deepest gratitude my mom Döne Yağmur, my uncle Ali Yağmur for their support.

Lastly, I would like to dedicate this work to my love Orhun Özyurt. Many thanks with all my heart for the most meaningful support.

2024, 25 November **Sidal YAĞMUR**

REMOVING METAL IONS FROM THE SOLUTION OF ELECTROPOLISHED KOVAR ALLOY

ABSTRACT

Electropolishing is a metal surface treatment technique, that involves the selective removal of particles from the metal's outer surface via the application of a controlled potential in an ionic solution. The aim of electropolishing is to obtain a smooth surface by removing ions on the metal surface in an appropriate solution to provide better performance parameters and improve the resistance of the parts against corrosion. However, the dissolution of metal ions during electropolishing leads to significant solution contamination, necessitating frequent replacement. This study focuses on collecting metal ions generated during Kovar alloy electropolishing onto a copper foil through electrodeposition, thus enabling the reuse of the electropolishing solution. Electrodeposition experiments were conducted using graphite or titanium anodes and copper foil cathodes. The optimal results were obtained with a voltage of 13 applied for 2 h, maintaining a pH of 3 at 25°C. This approach efficiently cleanses electropolishing solutions, fosters sustainable use and minimizing environmental impact.

Keywords: Electropolishing, Recycling electropolishing solutions, Mirror-Like Surface, Electrodeposition

ELEKTO PARLATILMIŞ KOVAR ALAŞIM ÇÖZELTİSİNDEN METAL İYONLARININ GİDERİLMESİ

ÖZ

Elektro-parlatma, iyonik bir çözelti içinde kontrollü potansiyelin uygulanması yoluyla metalin dış yüzeyinden parçacıkların seçici olarak uzaklaştırılmasıyla elde edilen bir metal yüzey işleme tekniğidir. Elektropolisajın amacı metal yüzeyindeki iyonları uygun bir solüsyonla gidererek pürüzsüz bir yüzey elde etmek, daha iyi performans parametreleri sağlamak ve parçaların korozyona karşı direncini arttırmaktır. Bununla birlikte, elektro-parlatma sırasında metal iyonlarının çözünmesi, çözeltinin önemli ölçüde kirlenmesine yol açarak sık sık değiştirilmesini gerektirir. Bu çalışma, Kovar alaşımının elektro-parlatılması sırasında oluşan metal iyonlarının, elektro-biriktirme yoluyla bir bakır folyo üzerine toplanmasına ve böylece elektro-parlatma solüsyonunun yeniden kullanılmasına odaklanmaktadır. Grafit veya titanyum anotlar ve bakır folyo katotlar kullanılarak elektrodepozisyon deneyleri yapıldı. 25°C'de pH 3 olan elektropolisaj çözeltisine 2 saat süreyle uygulanan 13 V potansiyel ile en iyi sonuçlara ulaşıldı. Bu yaklaşım, elektro-parlatma çözümlerini verimli bir şekilde temizlemeyi, sürdürülebilir kullanımı teşvik etmeyi ve çevresel etkiyi en aza indirmeyi vaat ediyor.

Anahtar Kelimeler: Elektro-parlatma, Geri dönüşüm elektro-parlatma çözümleri, Ayna Benzeri Yüzey, elektrodepozisyon

CONTENTS

NOMENCLATURE

Roman Letter Symbols

Zc	Electrochemical equivalent of the material
m	Coating mass
F	Faraday constant
ηeff	Efficiency

Greek Letter Symbols

μm	Micrometer
d	Density

Subscripts

A	Amper
I	Current
W	Weight
Qc	Coloumbs
T	Time
W	Cathode amount
M	Molecular weight
N	Oxidation state
A	Coated area

Acronyms

EP	Electropolishing
DC	Direct current
AC	Alternative current
HNO	Nitric acid
Cu	Copper
Ti	Titanium
Fe	Iron
Ni	Nickel
Co	Cobalt
C	Carbon
Si	Silicon
Mn	Manganese

LIST OF TABLES

LIST OF FIGURES

CHAPTER 1

INTRODUCTION

1.1 Kovar Alloy

Kovar is an alloy that was developed and patented in the USA in the early 1930s by CRS Holdings, a Delaware company. The name Kovar is derived from the first letters of the main ingredients it contains as shown in Table 1.1. Kovar is an alloy which consist of following quantities metals [1].

Table 1. 1 Chemical composition of Kovar Alloy[2]

The materials which is in Kovar alloy	**Composition of ingredients**
Fe	Balance
Ni	29%
Co	17%
C	<0,01%
Si	0,2%
Mn	0,3%

The role of the iron element in the Kovar alloy was to provide a matrix for the alloy. The iron content of 54% directly affects the magnetic properties of the material. The 17% cobalt percentage by weight in the alloy stabilizes the expansion properties of the material and provides strength. The weight control of 29% Ni element controls thermal expansion while also increasing corrosion resistance. Other than iron, nickel, and cobalt materials, like Mn, Si, and C increase the durability of the material, improve its melting properties, remove iron oxide, and control its grain structure, thus increasing its durability. From the late 1920s to the early 1930s, this valuable alloy was widely used in many industries, such as telecommunications, aviation, electronics, and medical fields. There are many avantages of its use, such as its low expansion coefficient, high compatibility with glass, and good mechanical strength. Some of these properties can be seen from the Table 2.

Table 1. 2 Properties of Kovar alloy [2]

Properties	**Metric**
Density	8,3 g/cm^3
Melting point	1449°C
Thermal conductivity	17,3 W/m-K

The above-mentioned advantages of Kovar alloy are frequently preferred in applications in which long life and precision are essential. Kovar alloy's thermal expansion rate (4.9 - 6.2 coefficient of thermal expansion (1 x 10^{-6}/°C)) aligns with that of borosilicate glass-ceramics, preventing damage during temperature changes, and maintaining integrity in a variety of thermal environments [3].

1.2 Electropolishing

Corrosion begins in areas close to the surface, and it damages surfaces immediately. The electropolishing process smoothens the surface and removes the damage caused by corrosion resistance. In this process, particles such as metal ions, grease, and dirt are dissolved from the metal surface [4]. Because of the process, a bright, and smooth surface is obtained, corrosion resistance is significantly improved and better performance is obtained. Electropolishing not only polish, deburring, welding, and spot cleaning, and passivation processes. With this process, the surface of the processed part is not damaged, and a metallurgical clean surface is formed. Electropolishing is a crucial process in industries with high corrosion resistance and cleanability.

The electropolishing process is used for almost all conductive materials such as stainless steel, titanium, copper, and alloys. Electropolishing is the most common chemical metal surface treatment technique. It is used to remove oxides, rust, and other impurities that arise from metals and alloys. In the electropolishing process, the material to be polished is called a positively charged anode. The cathode material, which is made of specially selected materials in contrast to the anode, is connected to the negative pole of a DC power source, and this process is carried out. The electric current passing through the DC power source is transmitted from the anode material to the cathode with the help of the electrolyte (solution). The electric current used in the process causes the metal ions on the surface of the part to oxidize and then dissolve in the electrolyte. During the process, a reduction reaction occurs on the surface of the cathode, producing hydrogen. There are many control parameters to perform this process. These are; chemical composition of the electrolyte, the capacity of the DC power supply, the test temperature of the electrolyte, the electropolishing time, the density of the applied electric current (A/cm^2), and the part on which the electropolishing process is targeted [5].

Electrolytic, chemical, and mechanical polishing methods are used to polish metal surfaces. The reasons why electropolishing is chosen over other methods include its relatively low cost, long lifetime, and applicability to complex geometries. In addition to these advantages, compared to traditional methods, the addition of electric current

to the electropolishing system allows greater control over the amount of metal removed from the surface down to micron sizes and a better finish surface [6].

1.3 Electropolishing of Kovar Alloy

Although the electropolishing process varies from application to application, it can be applied to materials such as aluminum, titanium, stainless steel, and various alloys. Kovar alloy, which contains iron, nickel, and cobalt, is one of them.

There are several main reasons why electropolishing is applied to Kovar alloys. The first step, as mentioned above, is to obtain better surface quality and higher performance by smoothing the alloy surface. Second, although the cover already exhibits good corrosion resistance, after electropolishing, a passive oxide layer is formed on the alloy surface, acting as a barrier. This further increases corrosion resistance.

1.4 Mechanism of the Electropolishing

As mentioned above, the polishing process can be performed manually (with the help of a polishing wheel machine), via electrochemical, chemical, or mechanical methods. The electropolishing process, which is frequently preferred for reasons such as its relatively affordable cost and its ability to be easily applied even to complex geometries, has been applied to different sectors since 1930. The electropolishing process provides a higher finish gloss compared to other techniques [7]. The basic working principle of the electropolishing process can be shown in Figure 1.1.

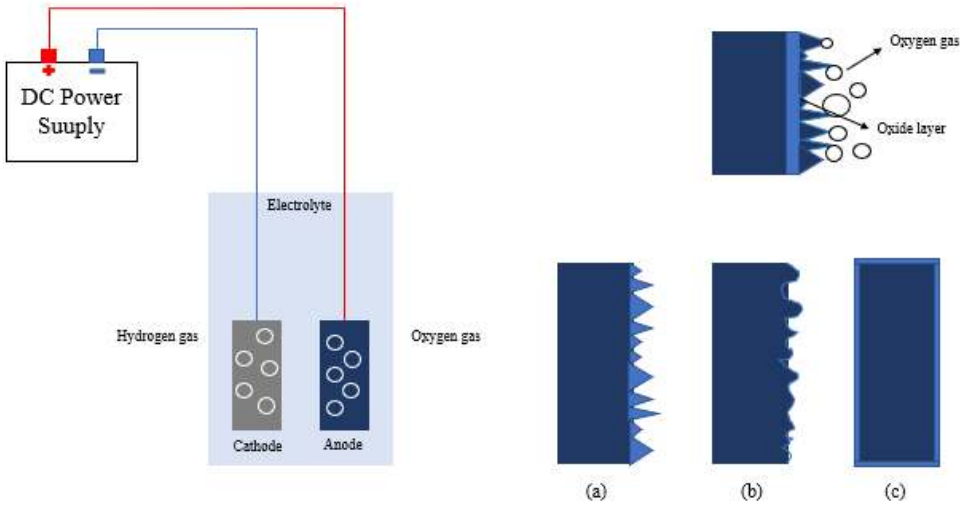

Figure 1. 1 The setup of an electropolishing process (a) Initial surface of the sample, (b) Macro-levelling surface, (c) Micro-levelling surface

In this technique, polishing of a metal or alloy part occurs in 2 stages. These; Smoothing, and Brightening [8].

During the first stage, smoothing, macroscopic irregularities on the surface of the electropolish part are eliminated. The scale used here is approximately 1 micron.

In the second stage, the polishing phase, small irregularities down to approximately 1/100 of 1 micron obtained in the first stage are eliminated [9]. In the image (a) in Figure 1.1, the initial irregular surface of the sample is visible. In (b), macro finishing is observed. Finally, in part (c), the surface obtained because of microfinishing is visible [10, 11].

The electropolishing technique can also be used to remove surface contaminants. The surface of a piece smoothed using the electropolishing method is shown in Figure 1.2. The part where electropolishing is performed serves as the anode. Therefore, it acts as a positive electrode. In this method, both the cathode and anode are connected to a power unit operating with DC current, and an electrical circuit is created in the electrolyte [12].

In this process, hydrogen and oxygen are supplied to the cathode and anode, respectively. It is expected that hydrogen embrittlement will not occur at the anode.

Because the anodic dissolution reaction occurs, only oxygen gas is released on the surface of the anode material [13].

No deterioration is expected on the metal or alloy surface after time has passed since the EP process [14].

Figure 1. 2 Images of the non-electropolished and electropolished samples [15]

It is obvious that the electropolishing process can be explained by the anodic polarization phenomenon in electrochemistry. The flow of current from the anodic region causes polarization of the anode in the electropolishing solution [12]. This process results in an anodic polarization curve that is typically based on changes in potential with the logarithm of current density or corrosion rate.

There are 3 main steps in a classical electropolishing process, they can be listed as follows.

1 . Preparation of the metal or alloy surface for the process to ensure the removal of all oils, lubricants, oxides. This preparation process can be performed using different methods. These methods include processes such as degreasing with vapor, cleaning the surface with acid, washing the metal or alloy in an ultrasonic bath, and sanding.

2. After the first stage of the operations, a second smooth and shiny surface.

3. Finally, after the processes are completed, the process of removing the chemicals/residues on the part surface [15].

The baths used in the electropolishing process generally consist of acid mixtures such as sulfuric acid, phosphoric acid, chromic acid, and perchloric acid. The main reason

for this is that acids do not provide conductivity so, anions dissolve. These acids are relatively hazardous to use and are therefore suitable for small-scale operations.

1.5 Metal Removal Techniques

During the electropolishing process, numerous metal ions are dispersed in the solution. Cleaning the solution from these ions is crucial for the environment, and the continuity, quality and performance of the electropolishing process. The direct or indirect disposal of heavy metals such as iron, nickel, and cobalt into nature is a very common situation, but it causes great harm to the environment. In addition to harming the environment, the metal ions left in solution significantly affect the quality, continuity, and performance of the next electropolishing process. Therefore, this problem must be solved. There are a wide variety of methods for metal recovery processes. Ion exchange, membrane technology, chemical precipitation, solvent extraction, acid swapping and cementation, adsorption and electrochemical treatment are some of these methods [16]. The electrodeposition method is frequently preferred due to its relatively affordable cost compared to other listed methods and its applicability in a wide variety of complex geometries. With the help of this method, the current coming from an external power source is passed through a solution called electrolyte, and the ions of the chemical bath containing ions are deposited/plated on a conductive surface, thus preventing solution pollution to a large extent [17].

1.6 Cell Types in Electrochemistry

Electrochemistry is a branch of science that studies the conversion of chemical energy into electrical energy or electrical energy into chemical energy. Different types of electrochemical cells were used to perform these conversions. There are two types of electrochemical cells that operate based on Faradaic current. These; They are galvanic (also called voltaic) and electrolytic cells [18].

When any electrochemical process is carried out, electrons are transferred from one chemical substance to another via a redox reaction. A redox reaction occurs when electrons are transferred from a substance that is being oxidized to a substance that is being reduced. In this reaction, the reductant loses electrons and is oxidized during the

reaction [19]. The other is called the oxidant and is the electron gainer. It is reduced during the process. Oxidation and reduction reactions occur in both cell types [20, 21].

1.6.1 Galvanic (Voltaic) Cell

Basically, a galvanic cell is called a device that converts chemical energy into electrical energy. These types of cells essentially contain only one electrolyte separated by a semiporous membrane. A more complex galvanic cell may contain two separate half-cells connected by a salt bridge [22]. While oxidation occurs at the anode, a reduction reaction occurs at the cathode. Because the current serves as the source of electrons for the reaction at the anode to occur, the anode is called the negative terminal of the galvanic cell [23].

The galvanic cell aims to produce electrical energy by using the energy released from the spontaneous redox reaction in which the Gibbs free energy change in the Gibbs system is negative. A schematic of the galvanic cell is shown in Figure 1.3 and equation's which belongs to the shematic are shown in equation (1.1), equation (1.2), and equation (1.3).

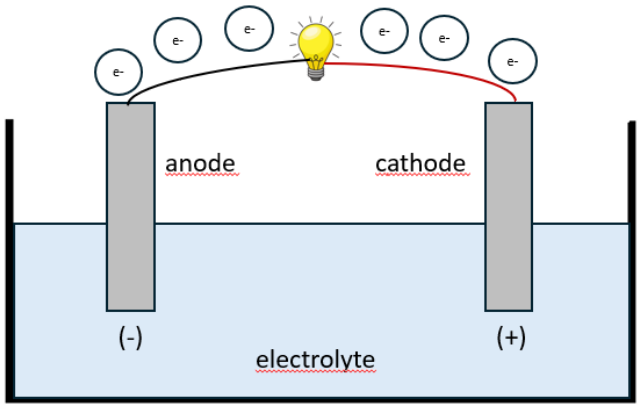

Figure 1. 3 Galvanic cell

Oxidation half reaction	$\mathrm{Y} = \mathrm{Y}^{+} + \mathrm{e}^{-}$	$(\mathbf{1.1})$
Reduction half rection	$Z^{+} + e = Z$	$(\mathbf{1.2})$
Overall cell reaction, G<0	$Y + Z = Y^{+} + Z$	$(\mathbf{1.3})$

1.6.2 Electrolytic Cells

Unlike the voltaic cell, the electrolytic cell is a device used to convert electrical energy into chemical energy. The electrolytic cell uses electrical energy produced from an external source as energy to produce a non-spontaneous redox reaction in which the Gibbs free energy change within the system is positive [24]. Essentially, it involves non-spontaneous reactions. Therefore, an additional DC battery or AC power supply is needed for the system to operate which can be seen in the Figure 1.4 [25]. Additionally, the reactions taking place in the electrolytic cell are given in equation (1.4), equation (1.5), and equation (1.6).

Since the reactions in the presence of oxygen gas occur slowly on the anode, the oxidation of the hydroxide is kinetically prevented [26, 27].

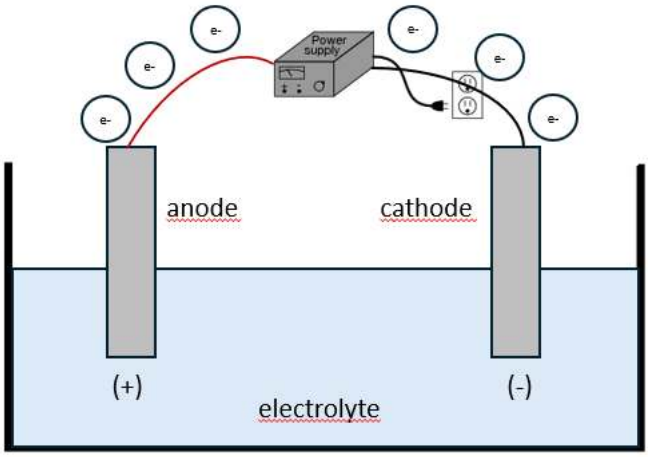

Figure 1. 4 Electrolytic cell

Oxidation half reaction	$\mathrm{Z} = \mathrm{Z} + \mathrm{e}$	$(\mathbf{1.4})$
Reduction half rection	$Y^{+} + e = Y$	$(\mathbf{1.5})$
Overall cell reaction, G>0	$Y^{+} + Z = Y + Z$	$(\mathbf{1.6})$

1.7 Electrodeposition

The discovery of the electrodeposition method emerged with the invention of the electric battery in the 1800s. This method is called the collection of metal ions in the solution on a different metal in the solution by applying current and voltage to the solution and the formation of a thin coating layer [28]. The principles of this process are fundamentally based on the electrochemical phenomena associated with the reduction/accumulation of electroactive, and companion species on the cathode material. The relatively low cost leads to the widespread use of this method [29].

Electrodeposition process is called an electrolysis process created by deposition of a metal piece or alloy on a conductive surface in an aqueous environment [30]. The metal deposited on the conductive surface is directly related to the chemistry of the solution it is in.

An electrolysis cell consists of components called anode, cathode, electrolyte/solution bath and external power supply [31]. The schematic of the process can be seen from Figure 1.5.

The anode serves as the electrode made of soluble or inert materials where the oxidation reaction can occur in the system. On the contrary of the anode, the cathode electrode is the part where the reduction reaction of the current applied to the system with the help of the power supply is carried out. The electrodeposition process occurs at the cathode electrode [32].

The scheme of the electrodeposition process looks as follows. During the process, first positively charged particles are formed in the electrochemical bath [33]. After these particles are formed, these positively charged particles are moved towards the cathode surface thanks to the mass transfer mechanism. Then, electrodes and particles interact in the electrolyte, and because of this interaction, the particles combine with the growing metal layers [34].

The main reason for performing this process is the recovery of metals in chemical solutions. While a recycling process is carried out for the solution, a coating is also obtained [35, 36].

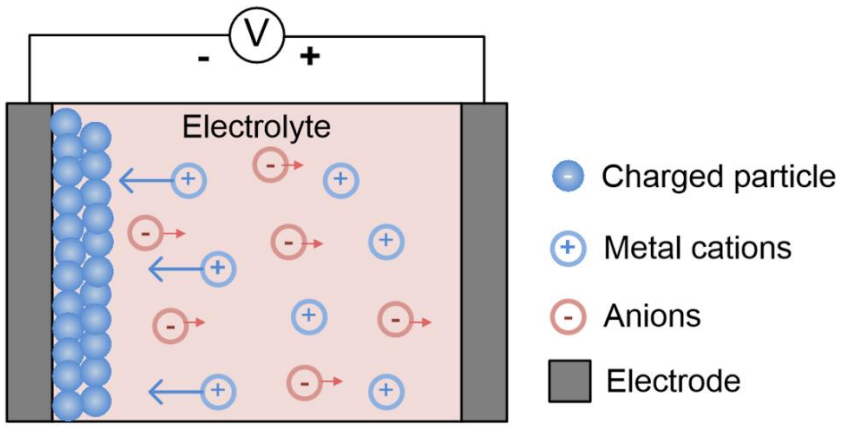

Figure 1. 5 Schematic of Electrodeposition process [37]

The electroplating process has many advantages, such as precise control over film thickness, improved surface properties, reduced environmental impact, and the ability to produce smooth/uniform coatings. The process is very important for the controlled deposition of each atomic layer within the material [38]. The method that allows this directly affects the film thickness. Controlling parameters such as current density, temperature and chemical composition of the electrolyte play an important role in the production of smooth and even coatings. In addition, mechanically strong final materials are obtained with the help of the electroplating method [39]. While the mechanical strength and surface properties of the materials are improved, they also increase their service life. Unlike other coating processes, the method does not have a negative impact on the environment [40, 41].

1.7.1 Fundamentals of Electrodeposition Process

The fundamentals of electrodeposition theory are directly related to Faraday's law. Faraday's law states the amount deposited at the cathode in grams (W), the total charge passing through the cell in coulombs (Qc), and the electrochemical equivalent of the metal (zc). These terms are shown in equation (1.7), equation (1.7a), and equation (1.7b).

$$W = \eta_{eff} \text{ x} \int M\ I\ \partial t/nF \qquad (\mathbf{1.7})$$

$$Qc = \int I\ \partial t \qquad (\mathbf{1.7}\boldsymbol{a})$$

$$z_c = M/nF \qquad (\mathbf{1.7}\boldsymbol{b})$$

The meanings of the parameters in the equation's above are;

I: It is the current value applied to the system and its SI unit is ampere.

T: is expressed in seconds and represents the elapsed time.

M: It refers to the molecular weight of the deposited metal.

N: indicates the total number of electrons reduced.

F: This value is Faraday constant (96.487 coulombs) (amp-sec)

ηeff: represents the efficiency value [42].

During the electrodeposition process, in addition to the cathode deposition reaction, hydrogen evolution reaction also occurs. As a result of this equation, hydrogen released. This released hydrogen causes the inefficiency of the process to increase. High current density results in increased hydrogen formation on the cathode side [43, 44].

1.8 Electrodeposition Parameters

There are many parameters that affect the electrodeposition process. These important parameters consist of things such as current density, electrolyte composition, temperature, anode or cathode material, and duration of the process to be performed. These important parameters play a very important role on the composition, stability and dissolution of the coating.

1.8.1 Current Density

It is a crucial parameter in the electrodeposition process due to the direct effect on mechanical properties such as tensile strength. Lower current density provides a smoother electropolishing finish surface. Increasing the current density may cause the material accumulated from the electrolyte bath to be unevenly coated on the cathode surface. This may result in a poor quality result [45].

The main reason for this inverse relationship is that the amount of current passing through the substrate affects the rate at which electrons move from the anode to the cathode. As the current density increases during the process, the electrons will start to move faster, thus decreasing the electroplating rate. In addition, the current density significantly affects the consistency of the electroplating. Increasing the current density can result in uneven coating. The main reason for this result is that the electrons move slower as the current density decreases and they have more time to spread evenly on the substrate of the materials. In addition to all of these, increasing the current density allows materials to be deposited more compactly and thicker, because current

density significantly affects the deposition rate and the amount of time it takes to spread before solidification.

The process can be carried out using direct, pulsed and pulsed reverse current methods. Direct current method is the oldest electrodeposition process method. The current value is continuously given to the system. This method is quite simple and applicable. It has been observed that the pulse current method increases the mechanical properties and homogeneity when compared to the direct current method. This method controls the microstructure and chemical content. In the pulse current method, pulse and peak current are called important parameters. The advantage of this technique is known as increasing the number of grains and coating in finer grain sizes. In the pulsed countercurrent method, a uniform coating deposition can be achieved. This method provides a reduction in internal stress compared to the direct current method.

1.8.2 Electrolyte Composition

The content of the electrolyte solution includes metal ions that accumulate on the cathode during electrodeposition. The content of this solution greatly affects the quality and thickness of the coating. During the electrodeposition process, the ion concentration in the electrolyte affects the rate of deposition of metallic ions and the efficiency of the deposited area. The ionic concentration in the solution has a direct effect on the process since it determines the number of charge carriers. The conductivity of the solution increases with the increase in the ion concentration. The increased solution conductivity results in increased current density without an increase in solution resistance. Excessive increase and excessive decrease of ion concentration value may cause some negativities. Therefore, a balance compatible with the process must be provided. If the balance is not provided, the mechanical properties and durability of the material are affected. In summary, a balanced ionic concentration ensures that the electrochemical reactions in the solution are strengthened and the targeted layer reaches the desired physical properties.

1.8.3 Anode and Cathode Materials

The correct selection of anode and cathode material affects the efficiency and quality of electrodeposition. The anode material to be selected must be compatible with the

electrolyte solution, and the cathode must have a good degree of conductivity. The selection of the correct anode and cathode materials has an effect on the process efficiency during the electrodeposition process. The determination of anode and cathode materials depends on properties such as corrosion resistance, mechanical properties, and electrical conductivity. In the electroplating process, the anode acts as the source of the reaction, while the cathode acts as the absorber of the reaction. The process efficiency depends on the redox potentials, solubility, and reactivity of the anode and cathode. The correct selection of these materials determines the speed and quality of the process. In addition, another effect of the appropriate selection of anode and cathode is on the electrolyte. And finally, the purity of the anode and cathode materials is very important for the process. If the impurities are at an unexpected level, this directly affects the process efficiency. If the purity is at the desired level, the electroplating speed and quality are obtained at the expected level.

1.8.4 Time

Duration of the electrodeposition directly affects the thickness of the coating. Increasing the time during the electrodeposition process is directly proportional to the greater accumulation of metal ions in the solution. In this way, more efficient results can be obtained by increasing the duration of the direct electrolysis process. The coating time is a very important parameter for the electroplating process to be efficient at the desired level. The coating time is directly related to the potential accumulation of the metallic layer. Although the increase in the coating time is directly proportional to the coating thickness, the uncontrolled nature of this time can have negative results. The decrease of ions in the electrolyte in a region close to the substrate surface can have negative results in the chemistry of the electroplating bath.

1.8.5 Physicochemical Parameters

The quality of the structural and optical properties of the coating on copper foil is directly related to parameters such as the conductivity of the solution, pH of the electrolyte and temperature. In addition to these parameters, ion concentration also serves as an important parameter in the electrodeposition process. Accumulation can be expressed as directly proportional to the number of ions [46].

The quality and thickness of the coating formed on the copper foil is directly proportional to the increase in the degree of conductivity and also the pH of the solution. At the same time, these important parameters directly affect the coating crystal. A decrease in pH value results in a decrease in current efficiency. Therefore, the efficiency of the coating process decreases with decreasing pH value. Since the decrease in solution pH will also decrease the amount of precipitation, it greatly affects the surface quality [45].

In addition, there is a direct relationship between conductivity and solution concentration. The higher the level of electrolyte conductivity, the better the result.

Temperature is another factor affecting the electrodeposition process. Carrying out this process at higher temperatures enables faster deposition/coating on the cathode. At the same time, uncontrollably increasing the temperature can also cause defects on the coating.

1.9 Measurement Technique

1.9.1 X-Ray Fluorescence (XRF)

XRF (X-Ray Fluorescence) is a characterization method frequently used in the qualitative and quantitative determination of the compositions of different material contents [47]. With the help of this method, elemental tests of solid, liquid, powder and mud materials can be performed. In addition to determining elemental compositions, it is also a frequently preferred method for measuring coating thicknesses formed on the cathode [48].

The working principle can be summarized as the samples to be analyzed absorb the X-ray fluorescence, excite the energy level of the X-ray from 1 to 2, and the device measures the emitted fluorescence and reduces the energy state from 2 to 1. The fluorescence that occurs during this process produces unique X-rays for each element [49]. The schematic image of this analysis is seen in Figure 1.6.

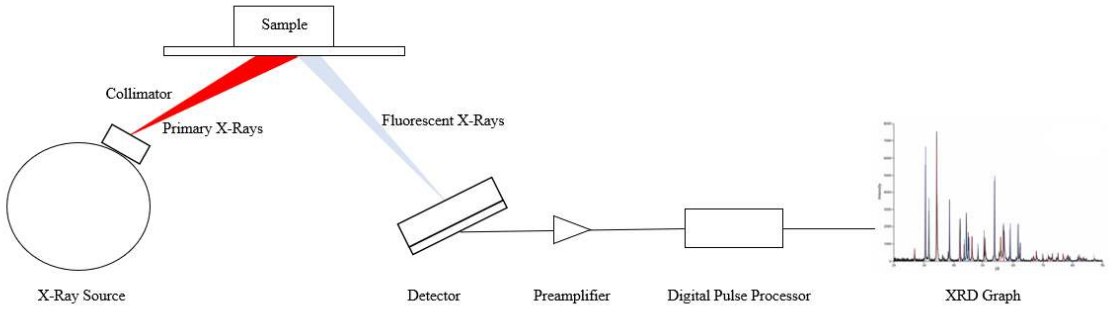

Figure 1. 6 Schematic Sequence of XRF Process

As can be seen from Figure 1.6, the system consists of few parts. When atoms are excited with high energy radiations such as X-rays, the high energy input carried out raises the orbits close to them to higher energy levels.

When the electrons excited in this way return to their initial energy levels, the excess energy on them emerges in the form of X-rays. The secondary X-ray emission that occurs here is called fluorescence radiation. The wavelengths of the radiation here are different for each element, just like a fingerprint, which provides a distinguishability. By determining the wavelength of the radiation here, the type of that element can be learned, and by determining its intensity, the concentration of that element can be learned [50, 51].

1.9.2 Inductively Coupled Plasma Emission Spectrometry (ICP-OES)

ICP-OES (Inductively Coupled Plasma-Emission Spectrometry) is known as a very sensitive and fast analytical technique that works for the determination of trace elements. With ICP-OES measurement, many elements such as alkali and alkaline earth elements, rare earth elements, many halogens, nonmetals can be analyzed with high scanning speed. Using this system, it is possible to obtain isotopic information about the elements and to perform multiple element analyses. What allows the person using the system to convert the elements to be analyzed first into atoms with the ICP source and then into ions is the combination of the system's inductively coupled plasma with a mass spectrometer. ICP-OES, which has a very wide usage, is quite popular in

the analysis of environmental, nuclear, chemical, geochemical, semiconductor and metallurgical applications.

Although solid analyses are also performed in the system, liquid analysis was performed within the scope of this study due to the thesis subject. The schematic image of this analysis is seen in Figure 1.7.

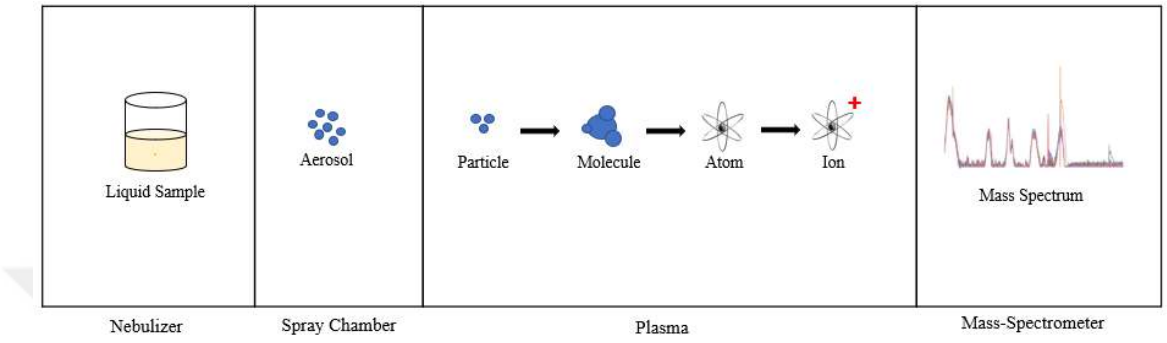

Figure 1. 7 Schematic Sequence of ICP-OES Process

The system basically consists of several parts. In the first part, the liquid sample is introduced into the device in aerosol form. The system basically consists of several parts. In the first part, the liquid sample is introduced into the device in aerosol form. The second part is called the ion production part. In this part, the aerosol sample is passed through a plasma consisting of argon flow, then dried, separated, vaporized and atomized. After all these processes, it is ionized by removing one electron from each atom due to the high temperature of the plasma. After these processes, there is the plasma/vacuum part of the system. In this part, positively charged ions are removed. The last part of the system is called the focusing part. In this part, ions pass through MS and photons, and the process of separating the ions from the remaining neutral substances is carried out. Here, the ions are detected and stored. As a result of all these processes, the ICP-OES analysis result is given with a spectrum [52]. The electrolyte contains 85% perchloric acid and 15% acetic acid. Since the large volume of perchloric acid in the solution damages the ICP-OES device, therefore in all ICP-OES measurements, the electrolytes were diluted 1000 times with pure water.

1.10 Aim of the Study

The aim of the study was to evaluate the removal of metal ions that can be observed in the electropolishing solution for Iron-Nickel-Cobalt alloy. In this process, it is also aimed to avoid wasting of the chemical solutions. In order to design a process in this context, laboratory-scale studies were carried out to determine the optimum current density, cathode, and anode materials.

CHAPTER 2

EXPERIMENTAL METHOD

The labrotary scale applications were performed for determining optimum current density, duration of electrolysis, and coating thicknesss for the collection of metal ions in the Kovar electropolished solution.

2.1 Characteristics of Electrolyte

It was aimed to recover the metal ions in the solution formed by the mixture of percloric acid (60%) and acetic acid, which are most commonly used in the electropolishing of Kovar alloy. The contents of the solution bath are given in Table 2.1.

Table 2. 1 Electropolishing electrolyte ingredients

Ingredients	Quantity
Acetic Acid	85%
Perchloric Acid (60%)	15%
Temperature	Room Temperature

2.2 Materials

Preliminary experiments were carried out to select suitable cathode and anode materials. As a result of these experiments, it was decided that the cathode material would be copper foil, considering its high conductivity. As for the anode, some of the experiments were carried out with graphite, while all the remaining experiments were carried out with titanium anode. As a result of the experiments, it was decided to continue the following experiments with a titanium anode because the graphite rod used as an anode dissolved in the solution consisting of a mixture of perchloric and acetic acid. No dissolution occurred when the titanium anode was immersed in the

solution. The set-up of the experiments which is carried out with copper foild cathode and titanium anode can be seen from the Figure 2.1.

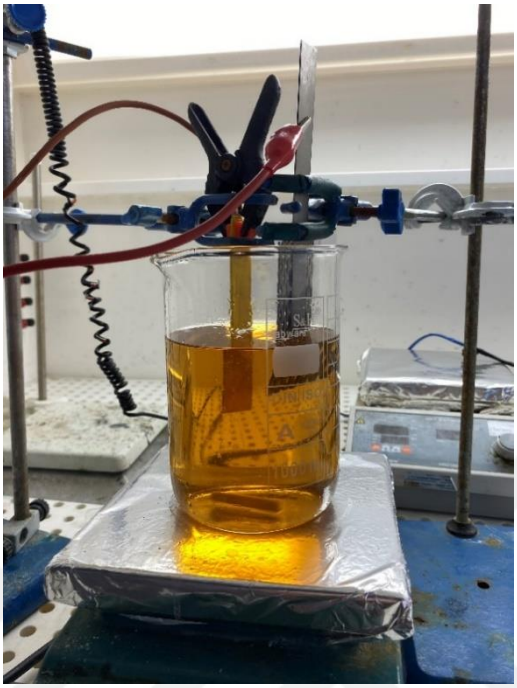

Figure 2. 1 Experiment set-up (Copper foil cathode and Titanium anode)

In order to decide on the correct anode to use, a graphite anode was used in addition to the experiments performed with the titanium anode. The experimental setup here is shown in Figure 2.2.

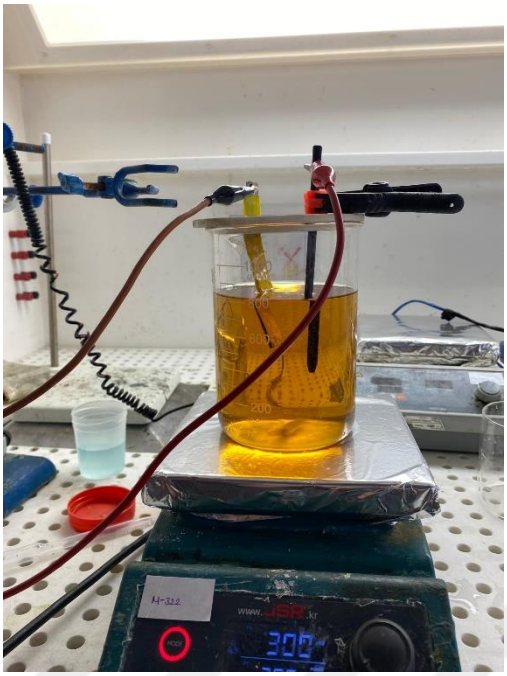

Figure 2. 2 Experimental set-up (Copper foil cathode and Graphite anode)

As a result of the experiments performed, when the samples taken from the solution were examined, it was seen that the graphite pieces were dissolved in the solution in the experiments performed with graphite anode, thus the test performance was seriously affected.

In addition to deciding the anode and cathode materials, in order to decide on the experimental parameters to be carried out within the scope of the thesis, potentiostat experiments were carried out at different scanning speeds by placing copper foil cathode and titanium anode materials in the solution before the experimental processes. As a result of these experiments, the voltage values at which electrodeposition experiments would be performed were decided.

2.2.1 Cathode Choice

Copper was used as the cathode material in this study because it has very good electrical conductivity, relatively affordable cost, ease of processing and good adhesion properties.

After the experiments, it was observed that working with copper cathodes required caution and that hot acid and acid vapor could quickly dissolve copper when not protected cathodically.

Figure 2. 3 Copper foil [53]

2.2.2 Cathode Preparation

Before each experiment, the cathode surface was cleaned with diluted nitric acid to remove particles such as dust and oil from the cathode surface in order to affect the experimental results and to perform a more accurate experiment. The cathode material copper foil, whose surface impurities were removed with nitric acid, was then rinsed with distilled water. This preliminary preparation process was carried out before each experiment. Nitric acid is a very strong acid and its chemical formula is HNO_3. Chemical formula of the HNO_3 can be seen from the Figure 2.4.

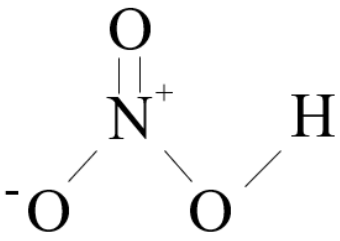

Figure 2. 4 Chemical formula of nitric acid

Since copper is a metal that reacts but does not react with dilute acids, nitric acid was chosen to clean copper within the scope of the study. Nitric acid is known as an

oxidizing acid. As a result of the reaction, azine oxides are formed in the output section. Copper nitrate, nitric oxide and water are formed as a result of the reaction of copper with dilute nitric acid. In this study, it was used only for the purpose of completely cleaning the copper surface [54].

To determine the weight gain and measure the coating thickness, the copper foils were weighed both with and without masks before the surface treatments. The same process was carried out after the experiment.

2.2.3 Anode Choice

The most important feature to consider when choosing the anode material in the electrodeposition system is that it consists of a material that will not dissolve in solution. As a result of the literature review, it was learned that it is possible to use cermet, lead, graphite, nickel and titanium as anode materials for electroplating. Titanium and graphite were examined as anode candidates under the same experimental conditions. As a result of the experiments, titanium was chosen as the anode material after evaluation of the results after characterization with XRF.

Titanium exhibits very good chemical stability even in aggressive electrolytes. At the same time, since they are an inert material, they do not enter into a chemical reaction with many substances under normal operating conditions.

2.2.4 Anode Preparation

In each experiment, graphite and titanium were first cleaned with acetone and then with distilled water to remove the dirt on the anode surface, as in the cathode material. Both of these processes were carried out with the help of an ultrasonic bath. In the last stage, the anode materials that were cleaned in an ultrasonic bath with water were left to dry and then the experiments were carried out. Chemical formula of the acetone can be seen from the Figure 2.5.

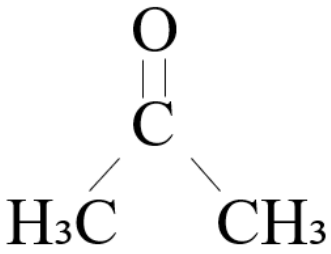

Figure 2. 5 Chemical formula of acetone

Acetone is often used to clean electrodes in experiments. Acetone has a low boiling point and can evaporate very quickly and easily clean contaminants, oils and residues on the surface, so it was used to clean the titanium anode in the study.

2.3 Experimental Set-up

In this study, the experimental setup was carried out using anode and cathode products placed in 700 ml of solution. The cathode of the electrodes was chosen as copper foil, the anode was chosen as graphite rod in a few experiments, and titanium in the other experiments. Although the coating surface area determined on the cathode was 8 cm^2 in the first few experiments, this area was reduced to 2 cm^2 in order to increase the coating efficiency as a result of a few experiments. The operating temperature in the experiments was 25 degrees centigrade.

The whole experimental set-up can be seen from the Figure 2.6.

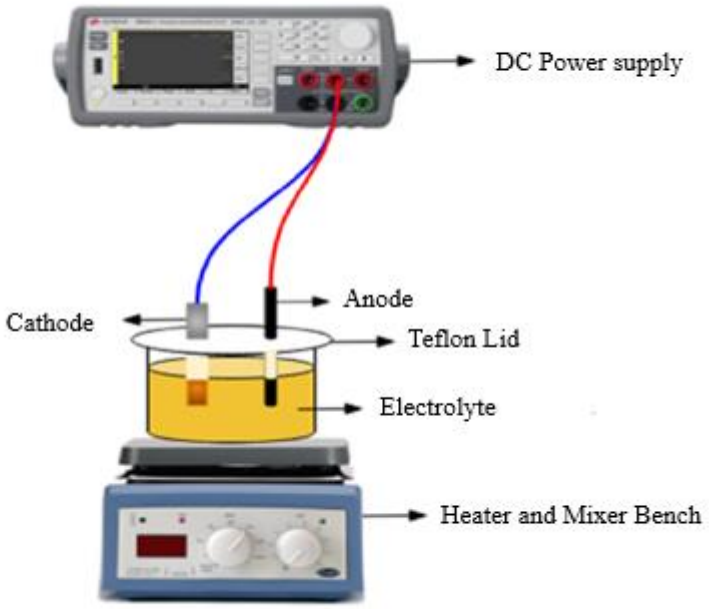

Figure 2. 6 Experimental set-up

The voltage value was determined as the working variable within the scope of the experiment. The experiments performed are given in the Table 2.2 with their parameters.

Table 2. 2 Carried out experiments

Anode	Cathode	Area (cm^2)	Time (h)	Voltage (V)	Average Current (A)
Titanium	Copper foil	8	1	1.5	0.0062
Titanium	Copper foil	8	1	2	0.0094
Titanium	Copper foil	2	1	2	0.0650
Titanium	Copper foil	2	1	5	0.2395
Titanium	Copper foil	2	1	8	0.4920
Titanium	Copper foil	2	2	8	0.4955
Titanium	Copper foil	2	3	8	0.4971
Titanium	Copper foil	2	1	11	1.0484
Titanium	Copper foil	2	1.5	11	1.0459
Titanium	Copper foil	2	3	11	1.0477
Titanium	Copper foil	2	1	12	1.1150
Titanium	Copper foil	2	1.5	12	1.2350
Titanium	Copper foil	2	1	13	1.3357
Titanium	Copper foil	2	2	13	1.3369
Titanium	Copper foil	2	3	13	1.3373
Titanium	Copper foil	2	1	15	1.4256

In addition to the tests performed which can be seen from Table 2.2, within the scope of the studies, pH and experimental temperature were kept constant. The pH of the solution was 3, and the experimental temperature was 25 degrees Celsius. In order to be able to make comparisons and comments after the experiments, only 1 variable was changed in each new experiment.

CHAPTER 3

RESULTS AND DISCUSSION

3.1 Choice of Electrodes

In the first experiments, an anode made of graphite rod and a cathode made of copper foil were used. When the samples taken from the first experiments were examined, it was determined that the particles of the graphite rod were disintegrate into the chemical solution consisting of perchloric acid and acetic acid. For this reason, it was decided that the cathode material to be used in the experiments within the scope of the study would be Cu. Addition to the cathode material, as mentioned in Section 2.2.3, Titanium was chosen as the anode material because it has a high chemical stability even in very aggressive solutions and its dissolution in the solution is small enough to be ignored.

3.2 Voltammetry Experiments

The most important factor in determining the current densities and time periods is the potentiostat experiments made before the experiment. The working principle of the potentiostat experiment is related to controlling the potential of a working electrode with respect to the reference electrode while measuring the current generated by the working electrode in the electrochemical cell. While the potentiostat keeps the potential of the electrode called the reference constant, a voltage is applied to the working electrode and a potential difference is created between this electrode and the reference electrode. The potential difference created directs the electrochemical reaction inside the cell and creates a current flow proportional to the reaction rate along the working electrode. Within the scope of the thesis, 6 different experiments were carried out with 25, 50 and 100 mV/sec scanning speeds. As a result of these experiments, the voltage ranges to be worked were determined. The results of the experiment carried out at scanning speeds of 25 mV/s is shown in Figure 3.1.

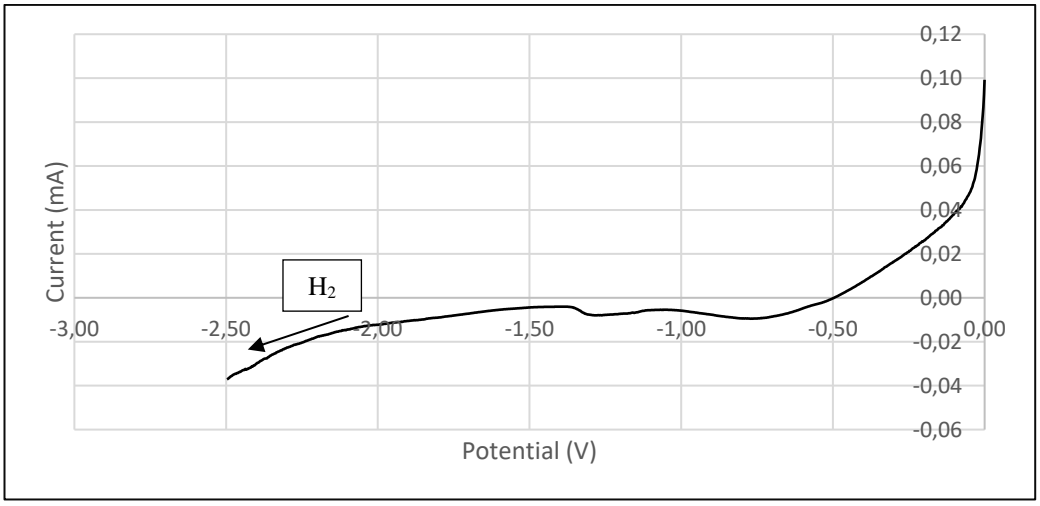

Figure 3. 1 Linear Scan Voltammetry of Electropolishing Solution Containing Kovar Alloy at 25 mV/s Scan Rate Using 2 cm2 Electrode Area

Figure 3.1 shows the linear sweep voltammogram of each Kovar electropolishing solution. By examining Figure 4.1, the potentials and corresponding current densities for the electrode reactions were obtained. As can be seen from the figure, at a potential difference of about -0.1 V between the anode and cathode, the first cathodic reaction started and gave reduction peaks at about -0.2 V, -0.3 V, and -0.45 V. These reduction peaks were attributed to the reduction of Ni^{+2} to Ni (equation (3.2)), Co^{+2} to Co (equation (3.3)), and Fe^{+2} to Fe (equation (3.4)), respectively. When the cathodic potential was further increased, a fourth and clear reduction peak was obtained at about -0.75 V, which was thought to be due to the reduction of $Co(OH)_2$ to Co and the formation of 2OH (equation (3.5)). And also, the hydrogen reduction reactin can be seen from the equation (3.1). When the cathodic current was slightly increased, the clearest reduction peak was obtained at -1.25 V. Starting from about -0.828 V and at later negative potentials, a lot of H_2 evolution was observed at the working electrode. The equations and corresponding potentials formed during the potentiostat experiments are given in Table 3.1.

Table 3. 1 Equations obtained from the potentiostat experiments at negative potentials performed with a scan rate of 25 mV/s

Potential (V)	***Equation***	
0	$2H^+ + 2e^- \rightarrow H_2$	$(\mathbf{3.1})$
-0,20	$Ni2^+ + 2e^- \rightarrow Ni$	$(\mathbf{3.2})$
-0,30	$Co2^+ + 2e^- \rightarrow Co$	$(\mathbf{3.3})$
-0,45	$Fe2^+ + 2e^- \rightarrow Fe$	$(\mathbf{3.4})$
-0,83	$H_2O + e^- \rightarrow \frac{1}{2}H_2 + OH^-$	$(\mathbf{3.5})$

When the results of the experiments carried out at different scanning speeds aiming for a smooth iron-nickel-cobalt deposition without too much H_2 evolution at the cathode were examined, it was decided to carry out the first experiments at low voltages such as 1.5 V and 2 V.

3.3 Effect of Applied Voltage

As mentioned in Section 3.2, when the potensiostat experiments are examined, the voltage value to be applied to the solution in the first experiments was determined as 1.5 V and 2 V.

XRF graphs of electrodeposition experiment performed in 1 hour at 1.5 is shown in Figure 3.2.

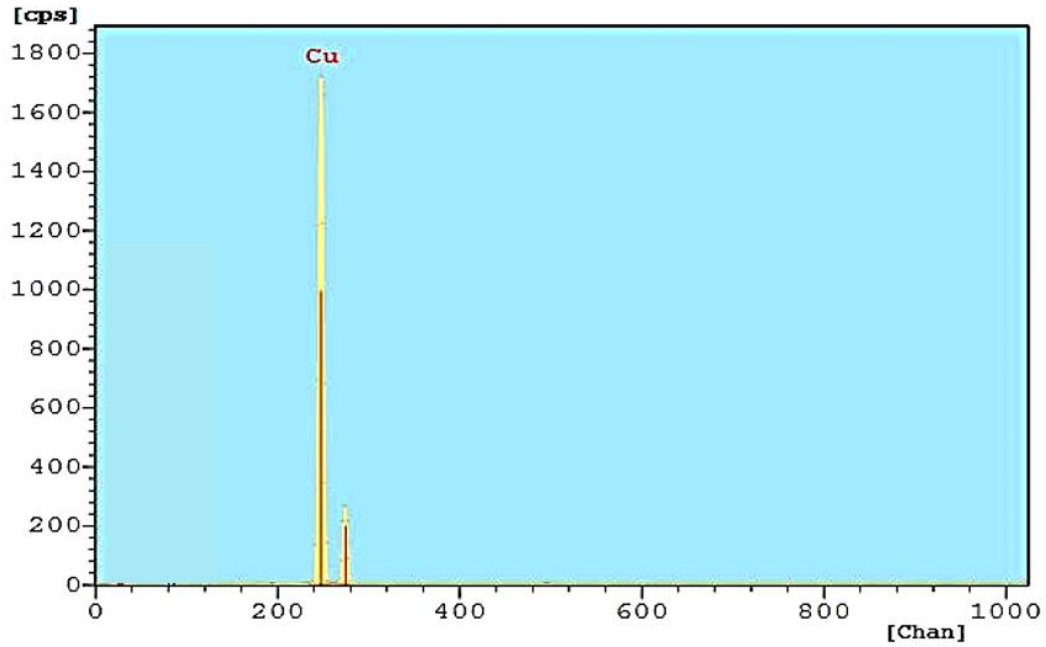

Figure 3. 2 XRF graph of electrodeposition experiment performed at 1.5 V for 1 hour on 2 cm^2 surface area

When the XRF taken from the coating on the copper cathode surface is examined which is Figure 3.2, it is seen that 100% copper was obtained as a result of the experiment. Subsequent experiments were carried out with 2, and 5 in order to collect the Fe, Ni and Co metal ions from the solution on the Cu cathode surface. 100% copper was found in the XRF measurements taken from the cathode surface of the electrodeposition experiments carried out for 1 hour at 2 and 5 volts. Since 100% copper was obtained in all experiments performed for 1 hour with 1.5, 2, and 5 V, the voltage value of the next experiment was increased further and performed with 8 V. The XRF graph of the electrodeposition experiment performed with the 8V, 1 hour, and 2cm^2 surface area conditions is shown in Figure 3.3.

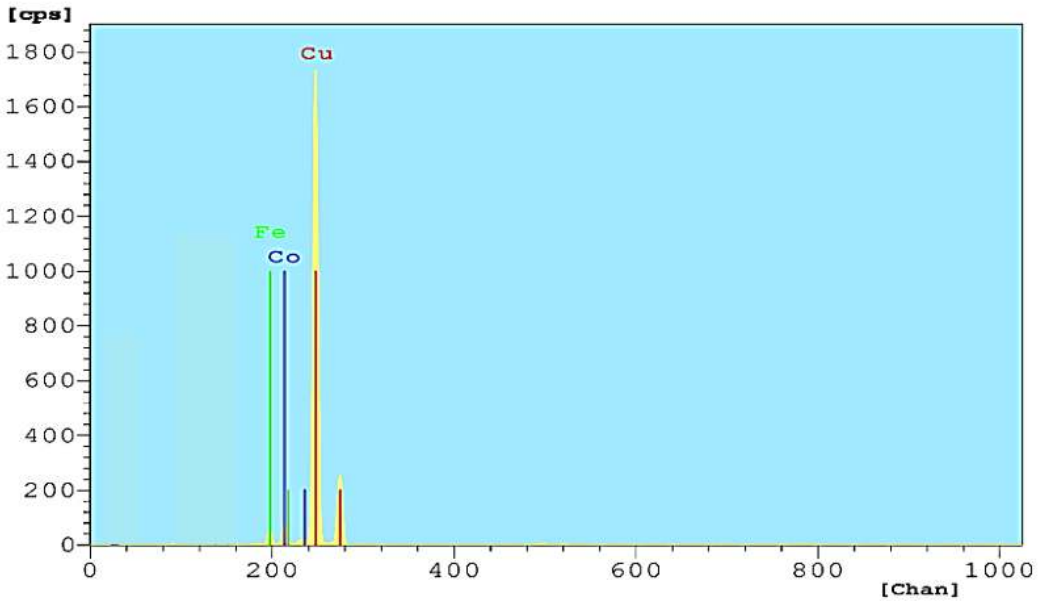

Figure 3. 3 XRF graph of electrodeposition experiment performed at 8 V for 1 hour on 2 cm2 surface area

As can be seen from Figure 3.3, Fe and Co metals were detected in the XRF result taken from the cathode surface as a result of the experiment carried out at 8 V for 1 hour. Another result showing that the experiment was successful which can be seen on the cathode surface in Figure 3.4. The color change on the cathode surface is due to the coating.

Figure 3. 4 Image of the cathode surface after the experiment performed at 8 V for 1 hour

When the results in Figure 3.3 and Figure 3.4 are examined, 54.16% of the coating on the copper surface was measured as Co and 45.83% as Fe by the help of XRF device. In this experiment performed at 8 V, the presence of Fe and Co metals, which are targeted to be found in the coating, shows the effect of increasing the voltage. In order

to collect more Fe, Ni, and Co on the cathode surface, experiments were carried out at 8, 11, 12, 13, and 15 V for 1 hour. XRF measurements were taken from each cathode surface in one-hour experiments carried out at the specified voltage values. The coating percentages on the cathode surface were also determined with the obtained XRF results. Figure 3.5 shows the voltage-dependent change in the iron concentration on the cathode surface in the experiments carried out for 1 hour at 8, 11, 12, 13, and 15 V values.

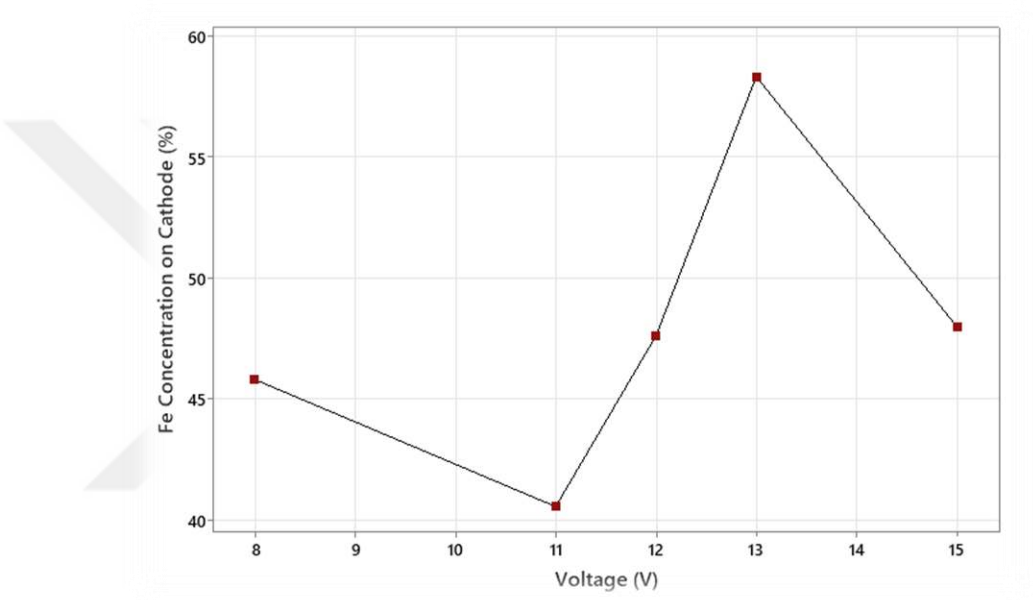

Figure 3. 5 Changes in the concentration of Fe in the coating during one-hour experiments at 8, 11, 12, 13, and 15 V

As can be seen from Figure 3.5, there was a net decrease in the iron concentration on the cathode surface in the 15V experiment following the experiment carried out with 13 V for 1 hour. In addition, there was a decrease in the iron concentration in the measurement taken from the cathode surface in the experiment carried out with 11 V. The reason for this is related to the fact that Ni metal was able to adhere to the copper cathode surface for the first time in this experiment.

According to Figure 3.5, the highest Fe concentration on the cathode surface was obtained from the experiments which is performed at 13V, 1 hour conditions. The XRF graph taken from the cathode surface of this experiment is shown in Figure 3.6.

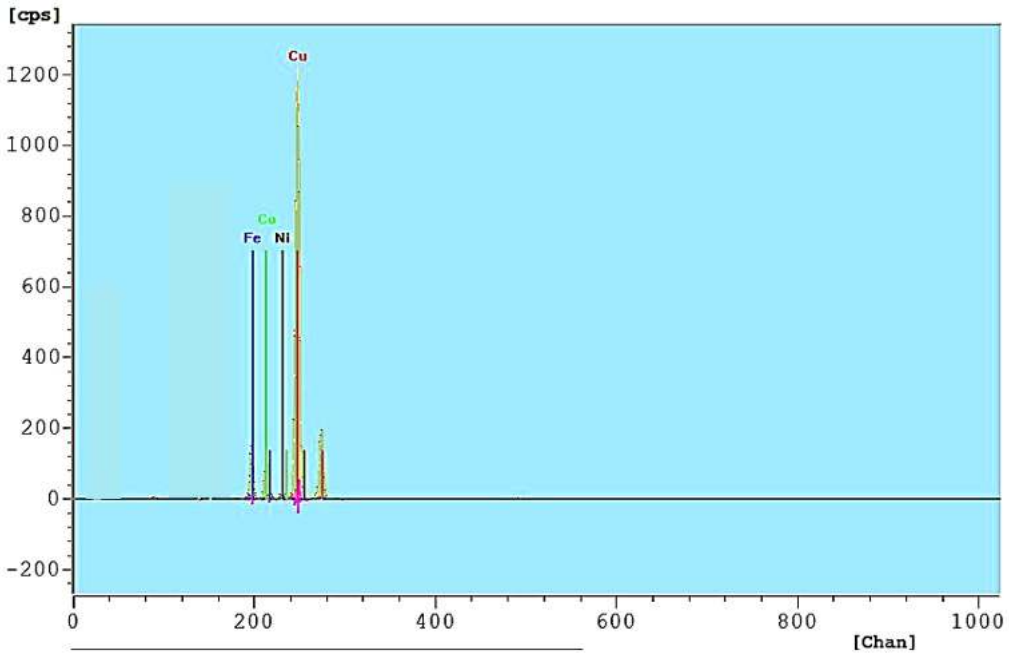

Figure 3. 6 XRF graph of electrodeposition experiment performed at 13 V for 1 hours on 2 cm2 surface area

As can be seen from Figure 3.6, the XRF device gave Fe, Ni, and Co peaks. The coating on the copper cathode surface consists of 58.34% Fe, 7.47% Ni, and 34.19% Co. In addition to the iron, nickel, and cobalt peaks, there is also copper peak seen in Figure 3.6, it comes directly from the base metal. Since copper is used as the cathode material, there is copper at the bottom of the coating area. Although the measurement is taken from the coating area on the copper foil, XRF also detects the copper material, which is the base metal under the coating.

In addition to XRF result of the experiment, the coating formed on the cathode surface after the experiment can be seen from the Figure 3.7.

Figure 3. 7 Image of copper foil cathode after the experiment performed 13 V, 1 hour, 2cm2 conditions

It can also be seen from Figure 3.7 that there is a metal coating formed on the copper foil surface. The color change is due to the coating formed on the cathode surface.
In addition to the calculation for Fe concentration, it was made same calculation for both nickel and cobalt metals and the result of the concentration calculation is given in Figure 3.8 and Figure 3.9, respectively.

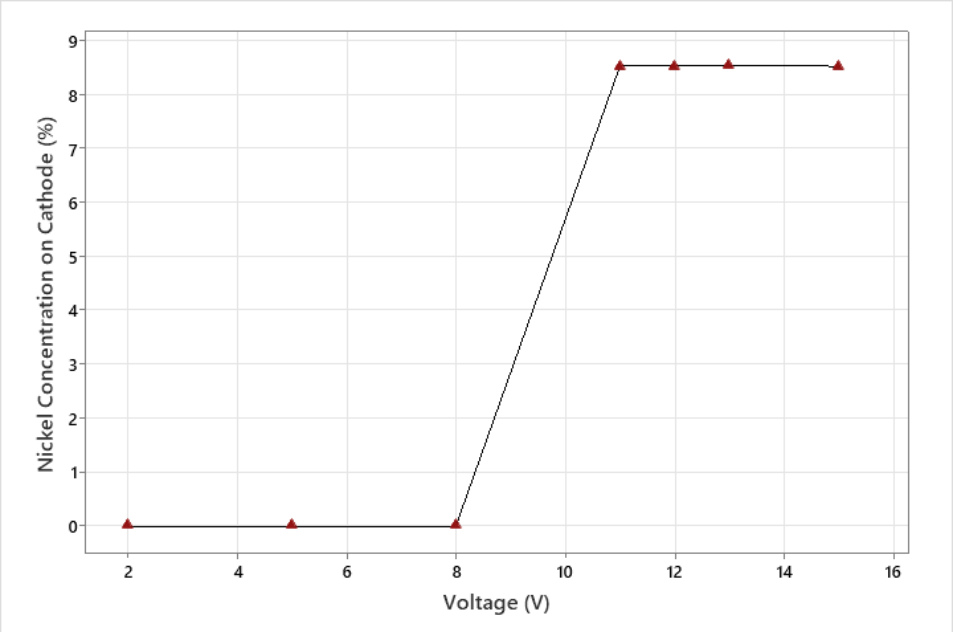

Figure 3. 8 Changes in the concentration of Ni in the coating during one-hour experiments at 8, 11, 12, 13, and 15 V

When Figure 3.8 is examined, Ni element wasn't found in the XRF measurements taken from the coating on the copper cathode surface in the experiments carried out for one hour at 2, 4, and 8 volts. In the experiment performed for 1 hour with 11 V potential, Ni metal was found in the coating for the first time. In the experiments after 11 V, the nickel ratio in the coating was preserved.

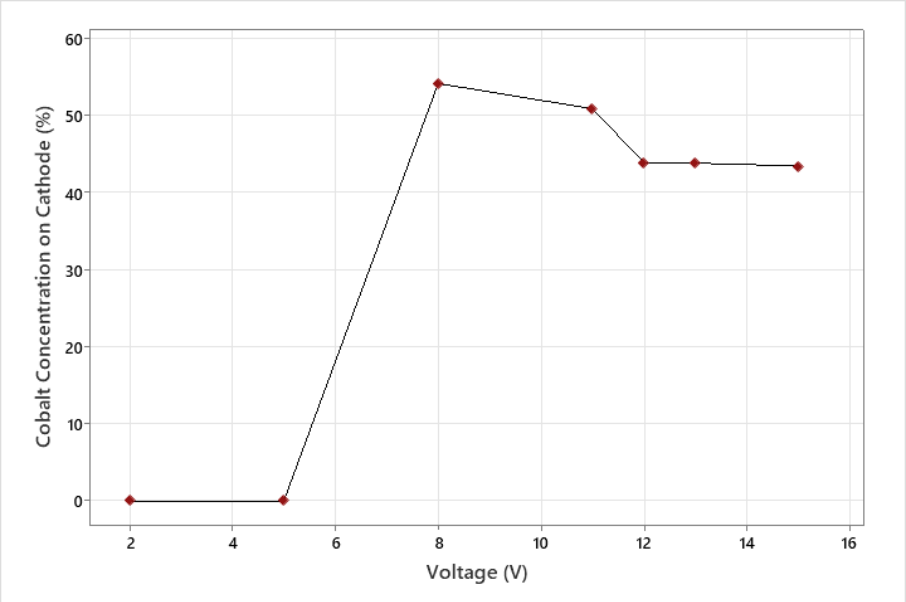

Figure 3. 9 Changes in the concentration of Ni in the coating during one-hour experiments at 8, 11, 12, 13, and 15 V

When Figure 3.9 is examined, Cobalt element was found in the coating on the cathode surface for the first time in the experiment performed at 8V. When the voltage value was increased by keeping the time constant, a decrease in Co concentration was observed as the Fe and Ni metal ions in the coating increased.

In addition to these results, the ICP-OES results obtained from the solutions in the experiments performed for 1 hour at 2, 8, 11, and 12 volts are shown in Figure 3.10.

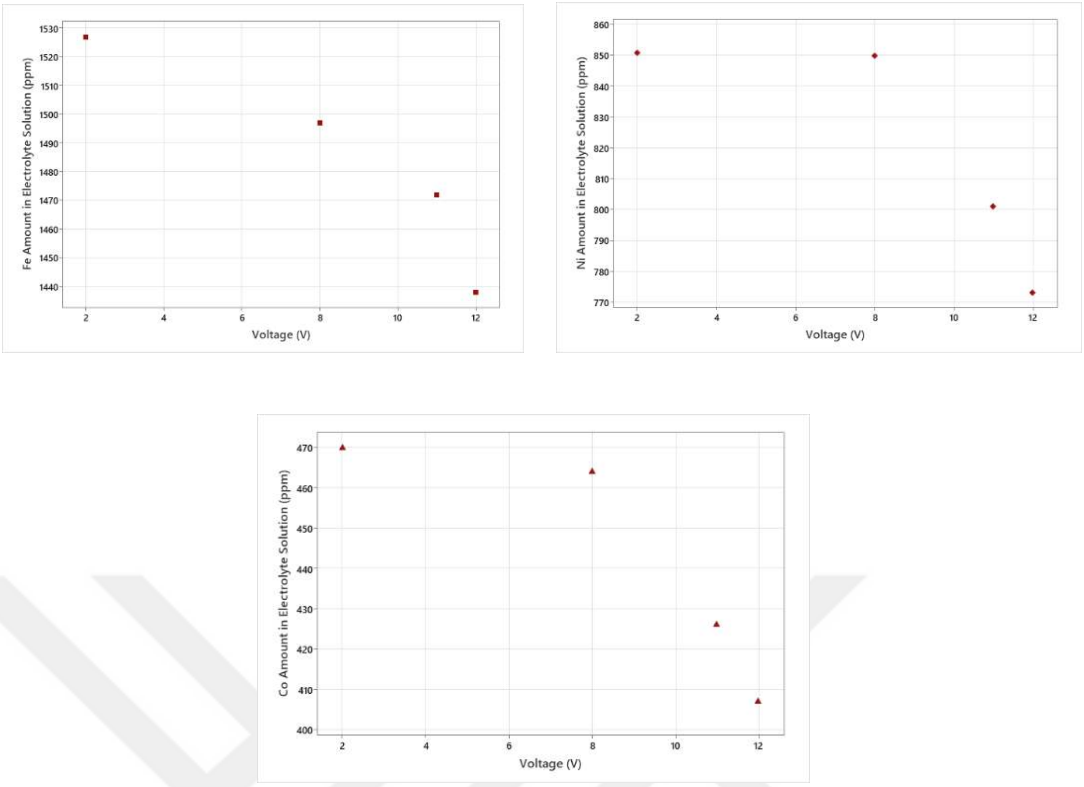

Figure 3. 10 The graph of Fe, Ni and Co metal ions change in the solution depending on voltage

As can be seen from Figure 3.10, as the voltage value increases (from 2 V to 12 V), there is a decrease in the Fe, Ni, and Co metal ions in the solution. This decreasing was a targeted result. Titanium metal was also detected in the ICP-OES device in addition to Fe, Ni and Co, but the amount of Ti measured in the solution was at levels of <0.01 ppm. Titanium anode was slightly dissolved in the solution.

3.4 Effect of Time

In order to see the effect of time within the scope of the study, experiments were carried out by keeping the voltage values constant and changing the electrodeposition durations variable for the experiments with the obtained high Fe, Ni, and Co concentrations on the cathode surface.

Within the scope of the study, 3 different experiments were carried out with 8V for 1, 2, and 3 hours. In order to clearly see the effect of time on the copper cathode, the measured weights were converted to coating thickness using equation (3.6).

$$\text{Coating Thickness } = 10000 \times \frac{\text{Weight}}{\text{Length} \times \text{Width} \times \text{Density}} \qquad (3.6)$$

where coating thickness is in micrometers, weight is in grams, length and width is in cm, and density is in g/cm^3 [56]. According to the equation (3.6), the change in the thickness of the coating on the cathode surface depending on the time as a result of the applied 8 V potential is shown in Figure 3.11.

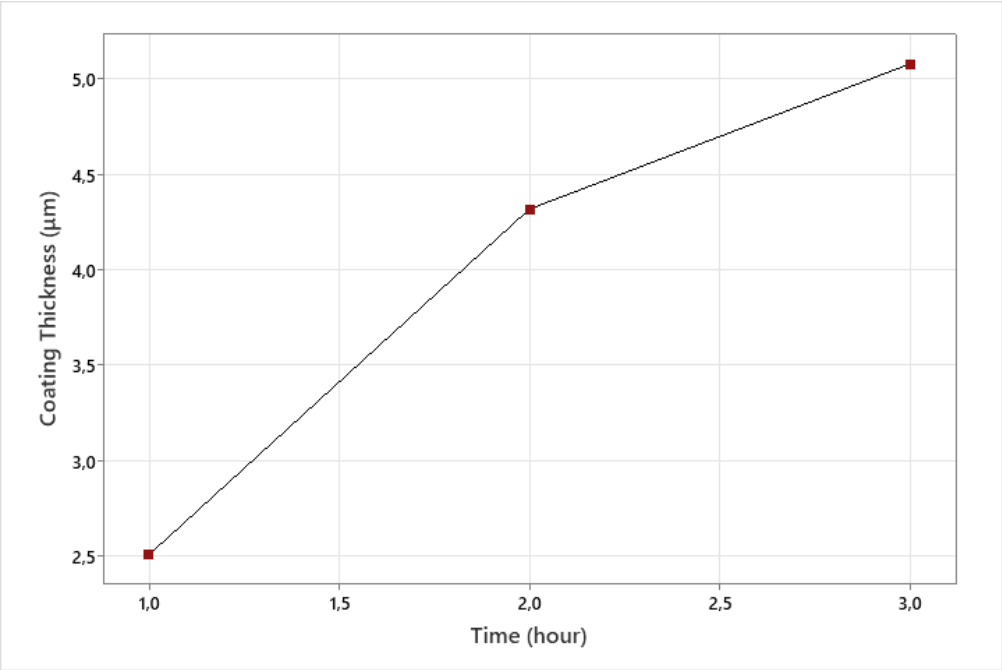

Figure 3. 11 The graph of coating thickness versus time in experiments performed with 8 V

When Figure 3.11 is examined, it is seen that when the electrodeposition time is increased while operating at constant voltage, the coating amount increases but the coating speed decreases. In addition to this result, the coating thickness was calculated by using the weight taken from the cathode surface using equation (3.6) at 13V. The graph shown in Figure 3.12 shows the coating thickness on the cathode surface calculated using equation (3.6) for 13V.

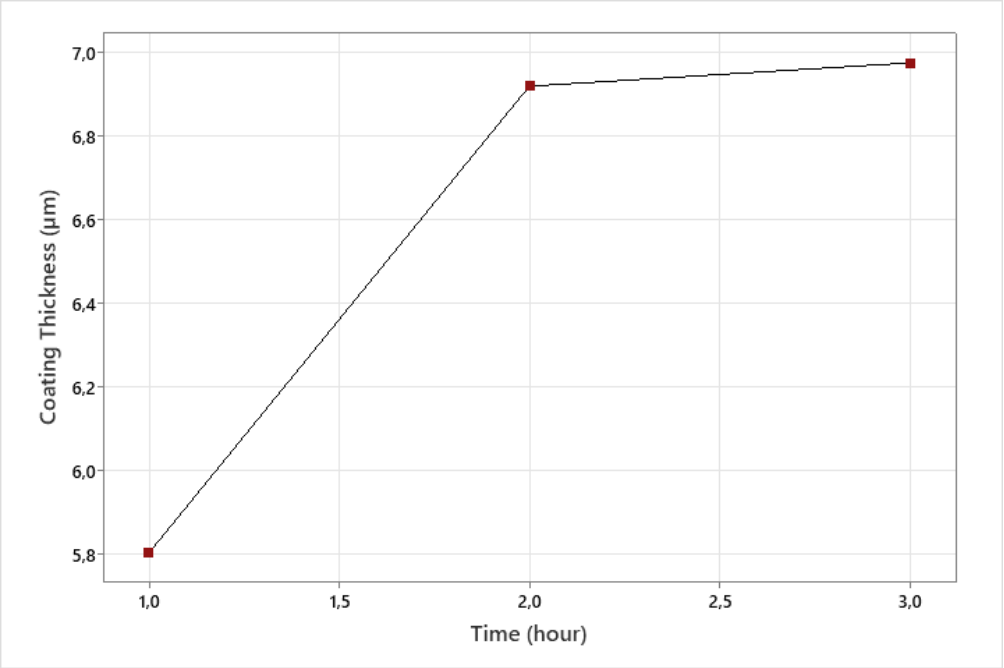

Figure 3. 12 The graph of coating thickness versus time in experiments performed with 13 V

It can be seen from Figure 3.10 that, as in Figure 3.12, when the test voltage is kept constant and the experiment duration is increased, the coating thickness increases while the coating speed decreases. It is clearly seen in Figure 3.12 that the coating thickness accumulated on the cathode surface reached 6.9196 micrometers as a result of the experiment which is performed during 2 hours. The XRF result taken from the surface of this experiment is given in Figure 3.13.

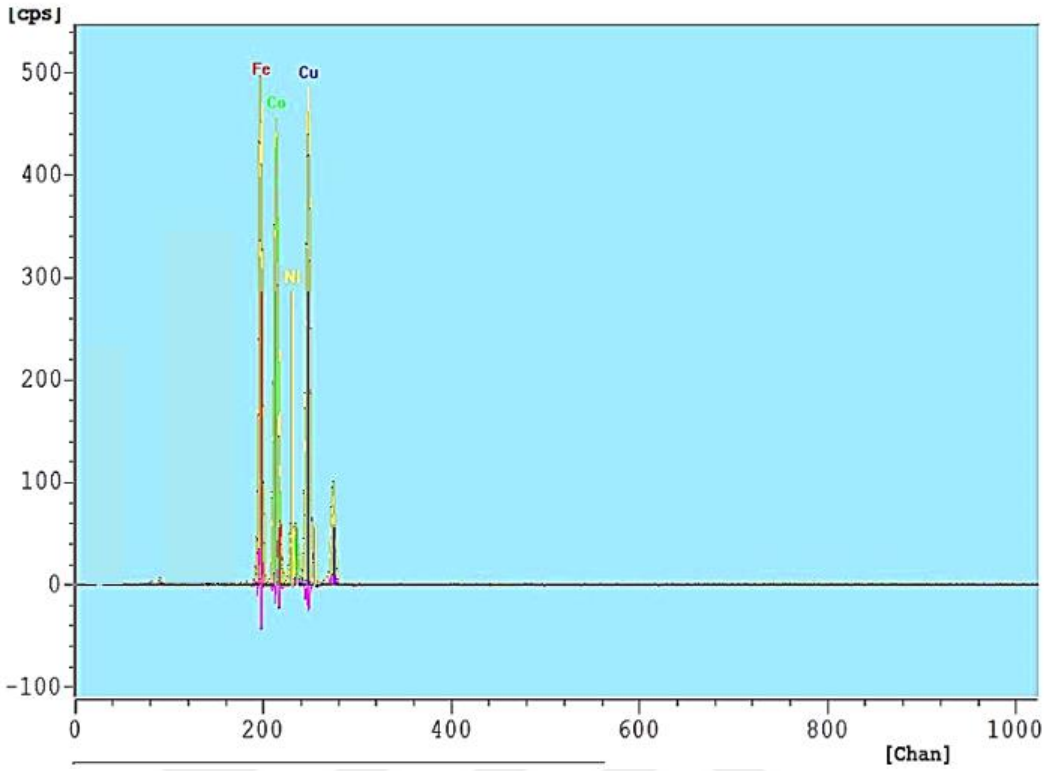

Figure 3. 13 XRF graph of electrodeposition experiment performed at 13 V for 2 hours on 2 cm2 surface area

When Figure 3.13 is examined, it is seen that Fe, Ni, and Co elements are collected on the Cu cathode surface. 48.97% of the coating formed on the cathode surface consists of Fe, 41.08% of Co and 9.95% of Ni. The copper peak in the XRF result is due to the cathode material being copper foil.

The coating thickness calculation was made using equation (3.6) for all performed experiments and these results can be seen from the Table 3.2.

Table 3. 2 Carried Out Experiments with Coating Thicknesses

Experiment Voltage (V)	**Coating Area (cm^2)**	**Experiment Duration (hour)**	**Weight (Before Exp.) (Grams)**	**Weight (After Exp.) (Grams)**	**Weight Difference (Grams)**	**Coating Thickness (µm)**
1.5	8	1	2.1599	2.1603	0.000	0.0558
2	8	1	2.2145	2.2151	0.000	0.0837
2	2	1	2.3342	2.3363	0.002	1.1719
5	2	1	1.9397	1.9424	0.003	1.5067
8	2	1	2.013	2.0175	0.005	2.5112
8	2	2	2.0211	2.0288	0.008	4.2969
8	2	3	1.4922	1.5013	0.009	5.0781
11	2	1	2.1066	2.1158	0.009	5.1339
11	2	1.5	1.5427	1.5523	0.009	5.3571
11	2	3	1.1889	1.1989	0.010	5.5804
12	2	1	1.8320	1.8421	0.010	5.6362
12	2	1.5	1.8239	1.8342	0.010	5.7478
13	2	1	1.8380	1.8484	0.010	5.8036
13	2	2	1.5959	1.6083	0.012	6.9196
13	2	3	1.7501	1.7626	0.013	6.9754
15	2	1	2.8793	2.8894	0.010	5.6362

When Table 3.2 is examined, the effect of time on the coating thickness is clearly seen in the experiments carried out at different durations with 8, 11, 12, and 13 volts. In all of these experiments (performed at 8, 11, 12, and 13 V) where the voltage was kept constant and the time was increased, it was seen that the coating thickness increased in direct proportion to the time.

In addition the coating thicknesses, the current values at the beginning, middle (when the current value reaches the steady state) and end of each experiment were noted. Figure 3.14 shows the current change with respect to time in the experiment performed by applying a 13 V potential during 2 hours.

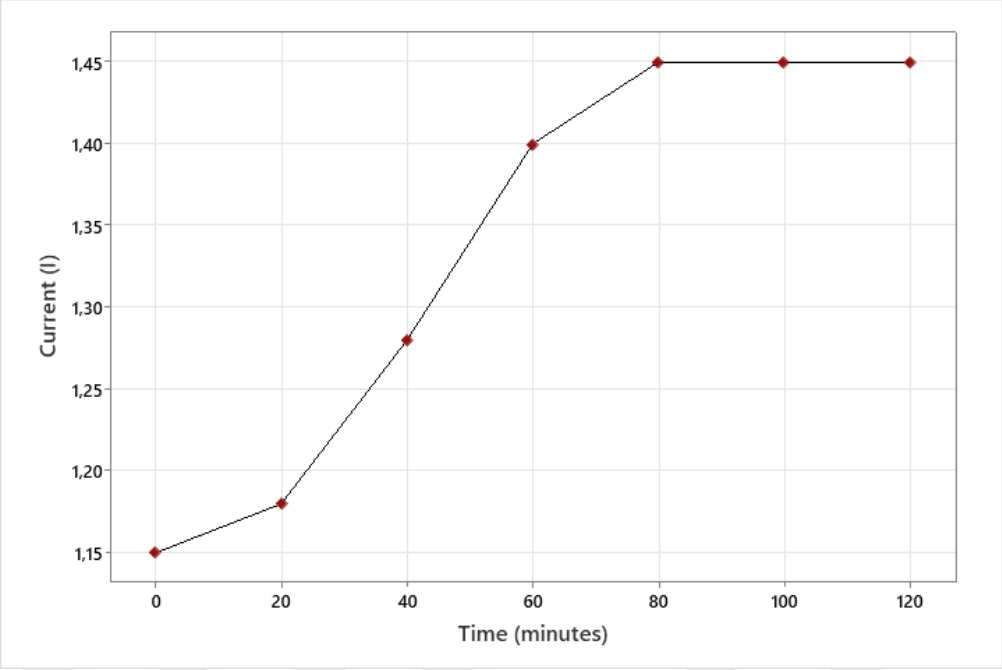

Figure 3. 14 Graph of the change of current over time in the experiment performed for 2 hours at 13 V

When the change graph of current with respecto to time at a constant voltage is examined in Figure 3.14, it is clearly seen that the current reached steady state in the 80th minute of the experiment. The current values specified in the thesis were calculated by taking notes at different times in the experiment and taking their averages, as shown in Figure 3.14.

3.5 Evaluation of Current Efficiency

Current efficiency is very important because it directly affects the success of an electrolytic process in converting electrical energy into chemical products. It is obtained by multiplying the ratio of the amount of substance produced as a result of the reaction to the charge passed by 100 (based on Faraday's law). The equation of the

current efficiency is shown in equation (3.7). The obtained value provides information about process performance, as well as how much of the current contributes to the conversion of the desired chemical and how much goes to side reactions. The electrode material, the concentration of the electrolyte, impurities, and the temperature value directly affect current efficiency.

$$\text{Current Efficiency} = \frac{\text{Actual mass}}{\text{Theoretical mass}} \times 100 \qquad (\mathbf{3.7})$$

The masses given in Equation (3.7) are in grams, and the current efficiency is expressed as a percentage [57, 58].

Current efficiency is also known as faradaic current. This term was first understood by the work of Michael Faraday and later began to be expressed in the laws of electrolysis. The theoretical mass which is given in equation (3.7) is expressed mathematically as in equation (3.8).

$$\text{Theoretical mass} = \frac{\mathrm{M} \times \mathrm{I} \times \mathrm{t}}{\mathrm{N} \times \mathrm{F}} \qquad (\mathbf{3.8})$$

where M in the equation represents molar mass, it's unit is g/mol, I represents the current flow in A, t represents the time in seconds, N represents the oxidation state, and F represents the Faraday constant [58].

The current efficiency was calculated for all of the performed experiment. These results can be seen from Table 3.3.

Table 3. 3 Carried Out Experiments with Current Efficiencies

Experiment Voltage (V)	**Coating Area (cm^2)**	**Experiment Duration (hour)**	**Weight Difference (Grams)**	**Current Efficiency (%)**
1.5	8	1	0.000	0.00%
2	8	1	0.000	0.00%
2	2	1	0.000	0.00%
5	2	1	0.000	0.00%
8	2	1	0.005	0.47%
8	2	2	0.008	0.39%
8	2	3	0.009	0.28%
11	2	1	0.009	0.39%
11	2	1.5	0.009	0.27%
11	2	3	0.010	0.15%
12	2	1	0.010	0.42%
12	2	1.5	0.010	0.25%
13	2	1	0.010	0.35%
13	2	2	0.012	0.21%
13	2	3	0.013	0.15%
1	2	1	0.010	0.33%

Table 3.3 shows the current efficiencies calculated using equation (3.7) and equation (3.8) for all experiments performed. When the current efficiency calculated in each experiment is subtracted from 100%, the remaining rate represents the rate of hydrogen output.

To see the effect of current efficiency on constant voltage and constant time, graphs were created based on Table 3.3. The graph showing the change of current efficiency with voltage while keeping the time constant at 1 hour is shown in Figure 3.15.

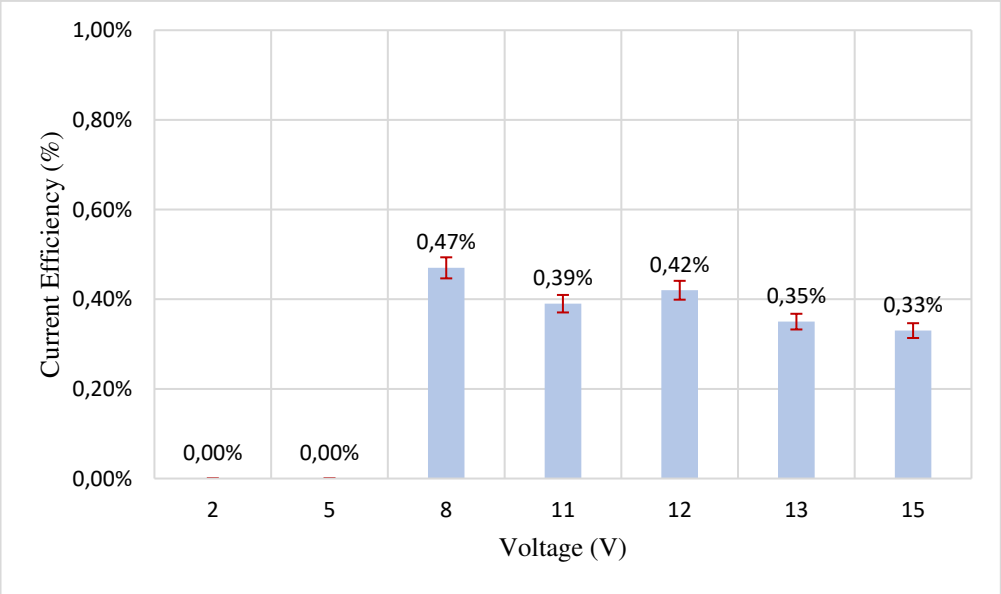

Figure 3. 15 Current efficiency versus voltage graph

Figure 3.15 shows that the highest current efficiency has been obtained at the 8V. In addition, coating thickness wasn't observed as a result of the experiments carried out with 2 and 5 V. Therefore, when 0 is put instead of actual mass in the equation (3.7), the current efficiencies become zero. The reason for the low current efficiency values is that the initial solution does not contain very high amounts of metal ions. In addition to the current efficiency - voltage relationship, Figure 3.16 shows the change in current efficiency over time in the experiments performed at constant voltage.

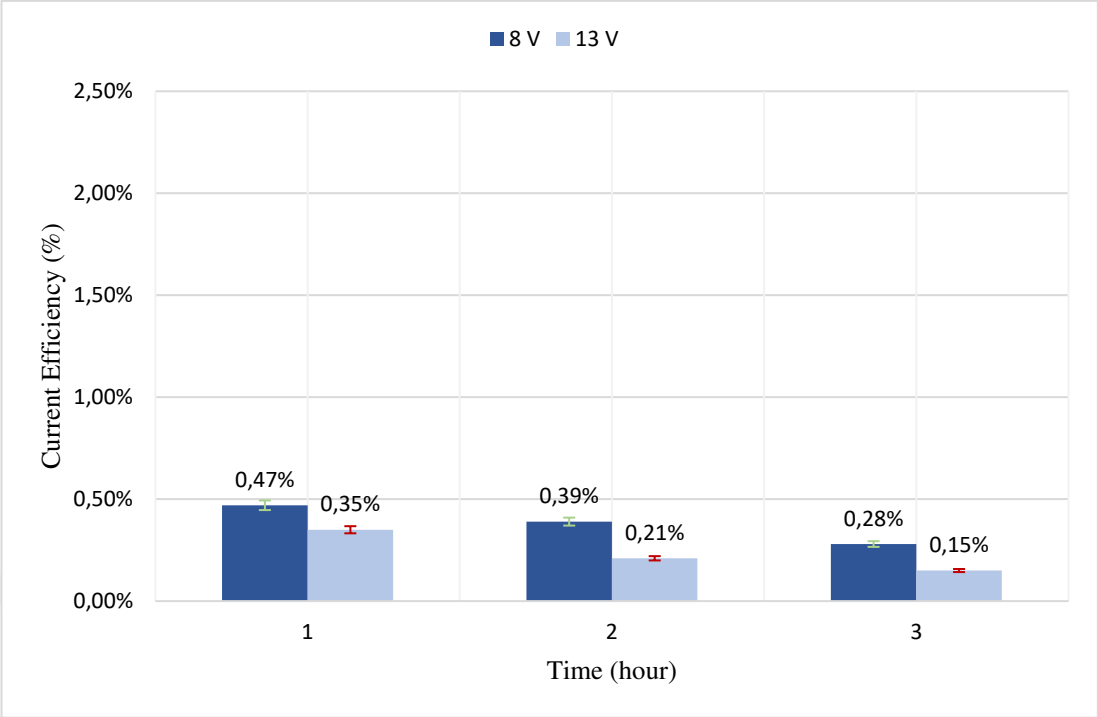

Figure 3. 16 Current efficiency versus time graph

Figure 3.16 shows the change in current efficiency in experiments performed at different times with potentials of 8 and 13 V. It is seen that when the duration of the electrodeposition process increases, current efficiency values decrease.

3.6 Evaluation of Energy Consumption

Calculating the energy efficiency of electrochemical processes plays an important role in the studies. It is obtained by dividing the total energy consumption in kWh by the mass of pollutant removed in kg. The total energy consumption is obtained by multiplying the voltage, current and time applied in the experiment and dividing the result by 1000. Equation (3.9) and equation (3.10) shows how total energy consumption is calculated.

$$\text{Energy Consumption} = \frac{\text{Total energy consumption in kWh}}{\text{Mass of pollutant removed in kg}} \qquad (\mathbf{3.9})$$

$$\text{Total Energy Consumption} = \frac{\text{Applied voltage} \times \text{Current} \times \text{Time}}{1000} \qquad (\mathbf{3.10})$$

The results are obtained by adding the current in A and the time in hours to the equation (3.10) [59, 60].

The energy consumption of the experiments carried out for 1 hour within the scope of the thesis was calculated using equation (3.9) and equation (3.10) and is given in Figure 3.17.

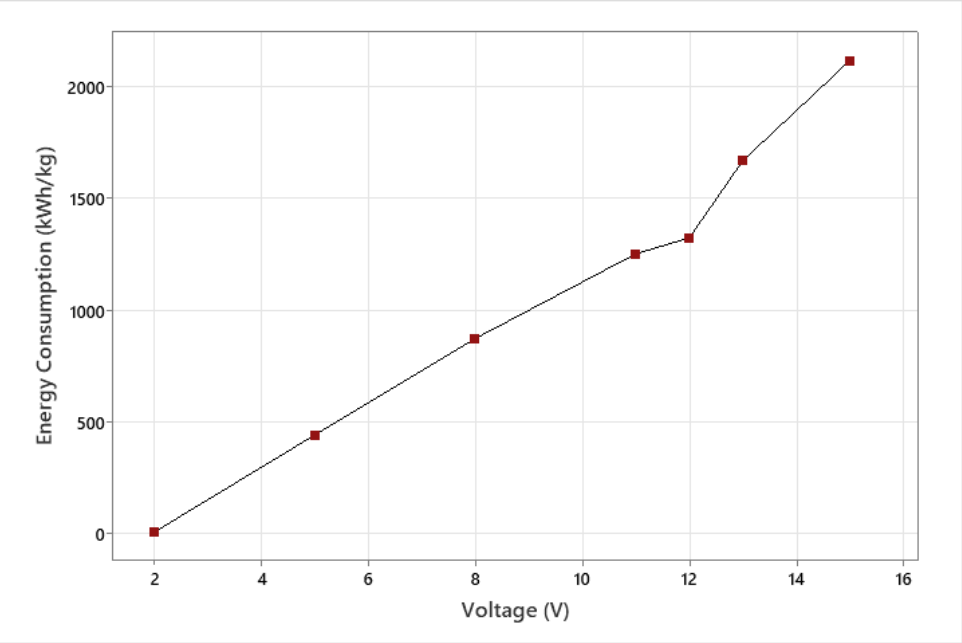

Figure 3. 17 Energy consumption versus voltage graph

When Figure 3.17 is examined, it is seen that energy consumption increases in direct proportion to the increase in voltage. In order to see the effect of time on energy consumption calculation, in addition to the voltage change, energy consumption calculations were made for experiments performed with 8 V and 13 V for 3 different times. The graph of energy consumption versus time is shown in Figure 3.18.

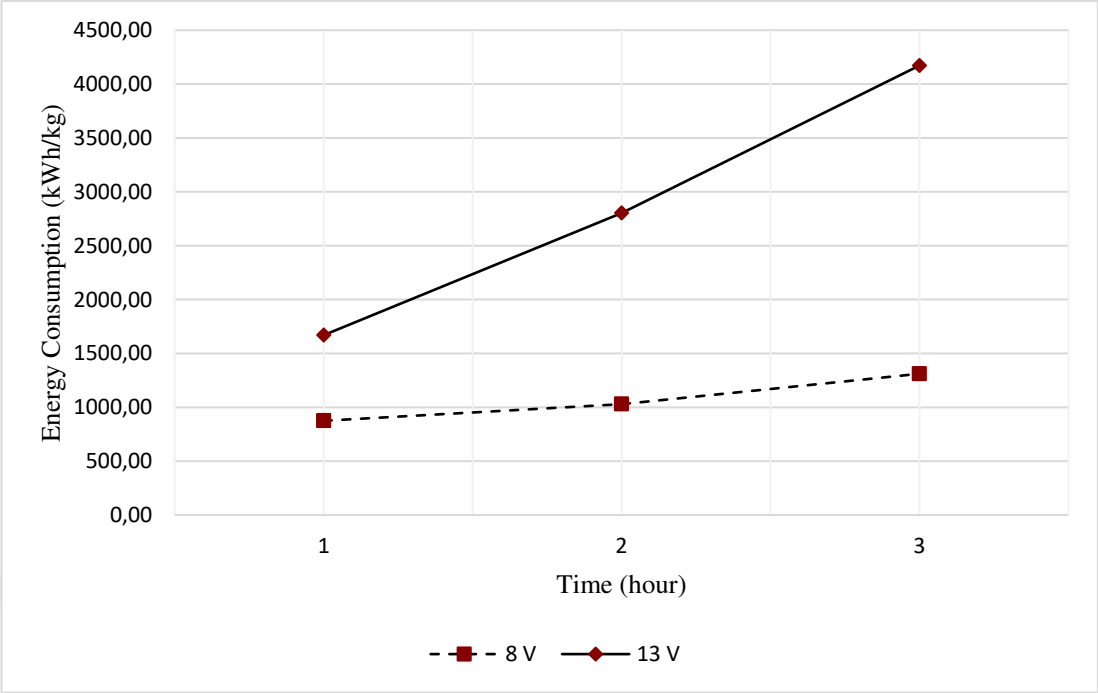

Figure 3. 18 The graph of energy consumption versus time

When Figure 3.18 is examined, energy consumption increases with increasing time in experiments of different durations performed with both 8 and 13 V.

CHAPTER 4

CONCLUSION

A metal alloy is deposited on a conductive surface in an aqueous environment to form the electrodeposition process, also known as electrolysis. It is a highly relevant process from a commercial standpoint, serving as the foundation for numerous industrial uses such metal plating, electrowinning, and refining. In addition, thanks to this process, metal ions can be collected on a cathode from large volume baths, as in this study, and bath cleaning and sustainability can be ensured.

In this thesis, the study's objective is to evaluate electrodeposition method for eliminating the metal ions that arise in the electropolishing solution for the Iron-Nickel-Cobalt alloy while also preventing chemical solution waste. The acid solution used in the experiments contained acetic acid and chromic acid mixture.

Graphite and then titanium were studied as the anode material because they provided the necessary stability in acidic solution. Copper foil was used as the cathode. The reason for using copper foil was that it had a high conductivity level. Within the scope of this study, the pH of the solution, the temperature of the electrolyte were kept the same, and the surface area for coating, the current density, and time values were changed. In the experiments, it was found that iron, nickel and cobalt metals were removed from the solution by increasing the current density and electrolysis time.

It was observed that the metal ions in the solution decreased as the current density and electrolysis time increased. When the XRF, weight differences, coating thicknesses, current efficiencies, and ICP-OES measurements of all experiments within the scope of the thesis are examined, it is seen that the optimum experiment performed within the scope of the thesis was the experiment carried out at 13V, 2 h, 2cm^2 conditions with a coating thickness of 6.9196 micrometers, a coating weight of 0.0124 grams, a current efficiency of 2.88%.

REFERENCES

[1] "The Uses and Uniqueness of Kovar - Eagle Alloys Corporation." Accessed: May 20, 2024. [Online]. Available: https://www.eaglealloys.com/the-uses-and-uniqueness-of-kovar/

[2] "Kovar Tech Data." Accessed: May 20, 2024. [Online]. Available: https://www.hightempmetals.com/techdata/hitempKovardata.php

[3] "Kovar | Mindrum Precision." Accessed: Aug. 15, 2024. [Online]. Available: https://www.mindrum.com/metal/kovar/

[4] W. Han and F. Fang, "Fundamental aspects and recent developments in electropolishing," *Int J Mach Tools Manuf*, vol. 139, pp. 1–23, Apr. 2019, doi: 10.1016/J.IJMACHTOOLS.2019.01.001.

[5] W. Han and F. Fang, "Fundamental aspects and recent developments in electropolishing," *Int J Mach Tools Manuf*, vol. 139, pp. 1–23, Apr. 2019, doi: 10.1016/J.IJMACHTOOLS.2019.01.001.

[6] Walter Schwartz, "Electropolishing," *Plating & Surface Finishing*, 2003.

[7] C. L. Faust, "Electropolishing—What is its Status to-day?," *Transactions of the IMF*, vol. 21, no. 1, pp. 181–288, Jan. 1945, doi: 10.1080/00202967.1945.11869455.

[8] Y. Aksu, M. Erdogan, G. Demirci, and I. Karakaya, "Electropolishing of an Fe-Ni-Co Alloy in Acetic Acid-Perchloric Acid Mixture," *ECS Meeting Abstracts*, vol. MA2016-01, no. 21, p. 1131, Apr. 2016, doi: 10.1149/MA2016-01/21/1131.

[9] D. Landolt, "Fundamental aspects of electropolishing," *Electrochim Acta*, vol. 32, no. 1, pp. 1–11, Jan. 1987, doi: 10.1016/0013-4686(87)87001-9.

[10] R. Hirate, M. So, G. Inoue, al -, S. Pourrahimi, and L. Hof -, "Review—Electropolishing of Additive Manufactured Metal Parts," *J Electrochem Soc*, vol. 169, no. 4, p. 043510, Apr. 2022, doi: 10.1149/1945-7111/AC6450.

[11] S. Zaki, N. Zhang, and M. D. Gilchrist, "Electropolishing and Shaping of Micro-Scale Metallic Features," *Micromachines 2022, Vol. 13, Page 468*, vol. 13, no. 3, p. 468, Mar. 2022, doi: 10.3390/MI13030468.

[12] S. Zaki, N. Zhang, and M. D. Gilchrist, "Electropolishing and Shaping of Micro-Scale Metallic Features," *Micromachines 2022, Vol. 13, Page 468*, vol. 13, no. 3, p. 468, Mar. 2022, doi: 10.3390/MI13030468.

[13] P. R. Rowland, "Mechanism of Electropolishing," *Nature 1953 171:4360*, vol. 171, no. 4360, pp. 931–931, 1953, doi: 10.1038/171931a0.

[14] I. Gavrila, "ELECTROLYTIC POLISHING OF METALS.," *Wireworld international*, vol. 24, no. 3, pp. 96–98, 1982, doi: 10.1080/00202967.1942.11869411/ASSET//CMS/ASSET/5FDBC0A0-2E92-4613-86C6-AEC73A88A780/00202967.1942.11869411.FP.PNG.

[15] Benu Chatterjee, *Science and Industry of Electropolishing*, vol. 71. Germany: Eugen G. Leuze Verlag, 2015.

[16] M. Yadav, G. Singh, and R. N. Jadeja, "Physical and Chemical Methods for Heavy Metal Removal," *Pollutants and Water Management: Resources, Strategies and Scarcity*, pp. 377–397, Jan. 2021, doi: 10.1002/9781119693635.CH15.

[17] M. Ince and O. K. İnce, "An Overview of Adsorption Technique for Heavy Metal Removal from Water/Wastewater: A Critical Review," *International Journal of Pure and Applied Sciences*, vol. 3, no. 2, pp. 10–19, Dec. 2017, doi: 10.29132/IJPAS.358199.

[18] P. J. Garnett and D. F. Treagust, "Conceptual difficulties experienced by senior high school students of electrochemistry: Electrochemical (galvanic) and

electrolytic cells," *J Res Sci Teach*, vol. 29, no. 10, pp. 1079–1099, Dec. 1992, doi: 10.1002/TEA.3660291006.

[19] M. Bekmezci, E. E. Altuner, V. Erduran, R. Bayat, I. Isik, and F. Şen, "Fundamentals of electrochemistry," *Nanomaterials for Direct Alcohol Fuel Cells: Characterization, Design, and Electrocatalysis*, pp. 1–15, Jan. 2021, doi: 10.1016/B978-0-12-821713-9.00023-8.

[20] "Enzymatic Fuel Cells: Materials and Applications - Google Kitaplar." Accessed: Aug. 15, 2024. [Online]. Available: https://books.google.com.tr/books?hl=tr&lr=&id=wdyEDwAAQBAJ&oi=fnd&pg=PA73&dq=electrochemistry+cell+types&ots=I7w4Mk9srW&sig=eTR3TE9qxEZxfOuUKKzSBy6btT0&redir_esc=y#v=onepage&q=electrochemistry%20cell%20types&f=false

[21] R. J. Marshall and F. C. Walsh, "A review of some recent electrolytic cell designs," *Surface Technology*, vol. 24, no. 1, pp. 45–77, Jan. 1985, doi: 10.1016/0376-4583(85)90015-9.

[22] K. E. Aifantis, R. V. Kumar, and Pu. Hu, "Rechargeable Ion Batteries Materials, Design, and Applications of Li-Ion Cells and Beyond.," 2022, Accessed: May 20, 2024. [Online]. Available: https://books.google.com/books/about/Rechargeable_Ion_Batteries.html?hl=tr&id=uLiYEAAAQBAJ

[23] P. J. Garnett and D. F. Treagust, "Conceptual difficulties experienced by senior high school students of electrochemistry: Electrochemical (galvanic) and electrolytic cells," *J Res Sci Teach*, vol. 29, no. 10, pp. 1079–1099, Dec. 1992, doi: 10.1002/TEA.3660291006.

[24] Stephen K. Lower, "Chemical reactions at an electrode, galvanic and electrolytic cells," 2004.

[25] R. J. Marshall and F. C. Walsh, “A review of some recent electrolytic cell designs,” *Surface Technology*, vol. 24, no. 1, pp. 45–77, Jan. 1985, doi: 10.1016/0376-4583(85)90015-9.

[26] A. A. Kulikovsky *et al.*, “DMFC: Galvanic or electrolytic cell?,” *Electrochem commun*, vol. 8, no. 5, pp. 754–760, May 2006, doi: 10.1016/J.ELECOM.2006.03.011.

[27] B. Andersson, “Pupils’ explanations of some aspects of chemical reactions,” *Sci Educ*, vol. 70, no. 5, pp. 549–563, 1986, doi: 10.1002/SCE.3730700508.

[28] W. Schwarzacher, “Electrodeposition: A technology for the future,” *Electrochemical Society Interface*, vol. 15, no. 1, pp. 32–33, Mar. 2006, doi: 10.1149/2.F08061IF/XML.

[29] I.-W. Sun and P.-Y. Chen, “Electrodeposition of Alloys,” *Electrodeposition from Ionic Liquids*, pp. 157–186, May 2017, doi: 10.1002/9783527682706.CH5.

[30] Abner Brenner, *Electrodeposition of Alloys*, vol. 1. New York and London, 1963.

[31] G. Z. Yuliy D. Gamburg, *Theory and Practice of Metal Electrodeposition*. 2011.

[32] Q. Zhang, Q. Wang, S. Zhang, X. Lu, and X. Zhang, “Electrodeposition in Ionic Liquids,” *ChemPhysChem*, vol. 17, no. 3, pp. 335–351, Feb. 2016, doi: 10.1002/CPHC.201500713.

[33] E. Gómez, J. Ramirez, and E. Vallés, “Electrodeposition of Co-Ni alloys,” *J Appl Electrochem*, vol. 28, no. 1, pp. 71–79, Jan. 1998, doi: 10.1023/A:1003201919054/METRICS.

[34] J. G. dos R. da Costa, J. M. Costa, and A. F. de Almeida Neto, “Progress on Electrodeposition of Metals and Alloys Using Ionic Liquids as Electrolytes,”

Metals 2022, Vol. 12, Page 2095, vol. 12, no. 12, p. 2095, Dec. 2022, doi: 10.3390/MET12122095.

[35] R. Winand, "Electrodeposition of metals and alloys—new results and perspectives," *Electrochim Acta*, vol. 39, no. 8–9, pp. 1091–1105, Jun. 1994, doi: 10.1016/0013-4686(94)E0023-S.

[36] R. Winand, "Electrodeposition of metals and alloys—new results and perspectives," *Electrochim Acta*, vol. 39, no. 8–9, pp. 1091–1105, Jun. 1994, doi: 10.1016/0013-4686(94)E0023-S.

[37] Esra Sütcü, "Copper Removal From Regenerated Pickling Solutions of Steel Plants," Middle East Technical University, Ankara, 2020.

[38] M. Nasim, Y. Li, M. Wen, and C. Wen, "A review of high-strength nanolaminates and evaluation of their properties," *J Mater Sci Technol*, vol. 50, pp. 215–244, Aug. 2020, doi: 10.1016/j.jmst.2020.03.011.

[39] G. Zangari, "Fundamentals of electrodeposition," *Encyclopedia of Interfacial Chemistry: Surface Science and Electrochemistry*, pp. 141–160, Jan. 2018, doi: 10.1016/B978-0-12-409547-2.11700-7.

[40] I. M. Dharmadasa and J. Haigh, "Strengths and Advantages of Electrodeposition as a Semiconductor Growth Technique for Applications in Macroelectronic Devices," *J Electrochem Soc*, vol. 153, no. 1, p. G47, 2006, doi: 10.1149/1.2128120.

[41] S. P. P. V. Sunil Kumar, "Factor Effecting Electro-Deposition Process," *International Journal of Current Engineering and Technology*, vol. 5, Apr. 2015.

[42] "Electrochemical cell, its working principle, setup and representation." Accessed: May 20, 2024. [Online]. Available: https://www.indiastudychannel.com/resources/144686-Electrochemical-cell-its-working-principle-setup-and-representation.aspx

[43] K. I. Popov, S. S. Djokić, N. D. Nikolić, and V. D. Jović, "Electrodeposition of Metals with Hydrogen Evolution," *Morphology of Electrochemically and Chemically Deposited Metals*, pp. 171–203, 2016, doi: 10.1007/978-3-319-26073-0_5.

[44] F. Nasirpouri, "Fundamentals and Principles of Electrode-Position," *Springer Series in Surface Sciences*, vol. 62, pp. 75–121, Jan. 2017, doi: 10.1007/978-3-319-44920-3_3.

[45] S. Kumar, S. Pande, and P. Verma, "International Journal of Current Engineering and Technology Factor Effecting Electro-Deposition Process," *International Journal of Current Engineering and Technology*, vol. 5, no. 2, 2015, Accessed: May 20, 2024. [Online]. Available: http://inpressco.com/category/ijcet

[46] M. Amiri and D. Bélanger, "Physicochemical and Electrochemical Properties of Water-in-Salt Electrolytes," *ChemSusChem*, vol. 14, no. 12, pp. 2487–2500, Jun. 2021, doi: 10.1002/CSSC.202100550.

[47] P. J. Potts and P. C. Webb, "X-ray fluorescence spectrometry," *J Geochem Explor*, vol. 44, no. 1–3, pp. 251–296, Jul. 1992, doi: 10.1016/0375-6742(92)90052-A.

[48] Peter Brouwer, *Theory of XRF*. Netherlands, 2010.

[49] V. P. Afonin, "X-ray fluorescence analysis," *Zhurnal Vsesoyuznogo Khimicheskogo Obshchestva imeni D.I. Mendeleeva*, vol. 25, no. 6, pp. 610–615, 1980, Accessed: May 21, 2024. [Online]. Available: http://inis.iaea.org/Search/search.aspx?orig_q=RN:13663787

[50] M. S. Shackley, "X-Ray Fluorescence Spectrometry (XRF)," *The Encyclopedia of Archaeological Sciences*, pp. 1–5, Jun. 2018, doi: 10.1002/9781119188230.SASEAS0620.

[51] A. Kumar Gupta, “Total Reflection X-Ray Fluorescence Spectroscopy-Working Principles,” *International Journal Of Core Engineering &Management (IJCEM)*, vol. 1, no. 5, 2014.

[52] V. Quang Do, “ONLINE MONITORING SYSTEM USING REACTOR AND MASS SPECTROMETRY in Can Tho,” 1984.

[53] “Copper Foil | Many Sizes | Shop Now at BasicCopper.com.” Accessed: Oct. 02, 2024. [Online]. Available: https://basiccopper.com/copper-sheets-and-rolls/1-mil-copper-foil/?srsltid=AfmBOooVqn-9aXZKBwDEHhcUIL23b7fdrhG7FywoMJjq5frHuz3YAJES

[54] A. S. A. E. B. R. K. C. 2 R. P. C. 1 R. K. M. S. M. C. M. P. W. K. N.-L. Jacquelyn M. Dorhout, “NOx Speciation from Copper Dissolution in Nitric Acid/Water Solutions Using FTIR Spectroscopy,” 2020.

[55] “How is Coating Thickness Measured? | Resources | DeFelsko.” Accessed: Nov. 08, 2024. [Online]. Available: https://www.defelsko.com/resources/coating-thickness-measurement

[56] “Calculate Plastic Film Thickness | Gauge By Weight Calculator.” Accessed: Nov. 09, 2024. [Online]. Available: https://www.gauging.com/customer-resources/film-calculators/calculate-film-thicknessgauge-by-weight/

[57] Ø. G. Martinsen and A. Heiskanen, “Electrodes,” *Bioimpedance and Bioelectricity Basics*, pp. 175–248, 2023, doi: 10.1016/B978-0-12-819107-1.00005-4.

[58] “Current Efficiency.” Accessed: Nov. 09, 2024. [Online]. Available: https://www.corrosionpedia.com/definition/355/current-efficiency

[59] “Energy Consumption Formula - Meaning, Calculation and FAQs.” Accessed: Nov. 09, 2024. [Online]. Available: https://www.vedantu.com/formula/energy-consumption-formula

[60] J. Rodziewicz, A. Mielcarek, W. Janczukowicz, and K. Bryszewski, “Electric Power Consumption and Current Efficiency of Electrochemical and Electrobiological Rotating Disk Contactors Removing Nutrients from Wastewater Generated in Soil-Less Plant Cultivation Systems,” *Water 2020, Vol. 12, Page 213*, vol. 12, no. 1, p. 213, Jan. 2020, doi: 10.3390/W12010213.